NASA/TP-2009-215561

Refined Zigzag Theory for Laminated Composite and Sandwich Plates

Alexander Tessler
Langley Research Center, Hampton, Virginia

Marco Di Sciuva and Marco Gherlone
Department of Aeronautics and Space Engineering
Politecnico di Torino, Torino, Italy

January 2009

NASA STI Program . . . in Profile

Since its founding, NASA has been dedicated to the advancement of aeronautics and space science. The NASA scientific and technical information (STI) program plays a key part in helping NASA maintain this important role.

The NASA STI program operates under the auspices of the Agency Chief Information Officer. It collects, organizes, provides for archiving, and disseminates NASA's STI. The NASA STI program provides access to the NASA Aeronautics and Space Database and its public interface, the NASA Technical Report Server, thus providing one of the largest collections of aeronautical and space science STI in the world. Results are published in both non-NASA channels and by NASA in the NASA STI Report Series, which includes the following report types:

- TECHNICAL PUBLICATION. Reports of completed research or a major significant phase of research that present the results of NASA programs and include extensive data or theoretical analysis. Includes compilations of significant scientific and technical data and information deemed to be of continuing reference value. NASA counterpart of peer-reviewed formal professional papers, but having less stringent limitations on manuscript length and extent of graphic presentations.

- TECHNICAL MEMORANDUM. Scientific and technical findings that are preliminary or of specialized interest, e.g., quick release reports, working papers, and bibliographies that contain minimal annotation. Does not contain extensive analysis.

- CONTRACTOR REPORT. Scientific and technical findings by NASA-sponsored contractors and grantees.

- CONFERENCE PUBLICATION. Collected papers from scientific and technical conferences, symposia, seminars, or other meetings sponsored or co-sponsored by NASA.

- SPECIAL PUBLICATION. Scientific, technical, or historical information from NASA programs, projects, and missions, often concerned with subjects having substantial public interest.

- TECHNICAL TRANSLATION. English-language translations of foreign scientific and technical material pertinent to NASA's mission.

Specialized services also include creating custom thesauri, building customized databases, and organizing and publishing research results.

For more information about the NASA STI program, see the following:

- Access the NASA STI program home page at *http://www.sti.nasa.gov*

- E-mail your question via the Internet to help@sti.nasa.gov

- Fax your question to the NASA STI Help Desk at 443-757-5803

- Phone the NASA STI Help Desk at 443-757-5802

- Write to:
  NASA STI Help Desk
  NASA Center for AeroSpace Information
  7115 Standard Drive
  Hanover, MD 21076-1320

NASA/TP-2009-215561

Refined Zigzag Theory for Laminated Composite and Sandwich Plates

Alexander Tessler
Langley Research Center, Hampton, Virginia

Marco Di Sciuva and Marco Gherlone
Department of Aeronautics and Space Engineering
Politecnico di Torino, Torino, Italy

National Aeronautics and
Space Administration

Langley Research Center
Hampton, Virginia 23681-2199

January 2009

Available from:

NASA Center for AeroSpace Information
7115 Standard Drive
Hanover, MD 21076-1320
443-757-5802

Abstract

A refined zigzag theory is presented for laminated-composite and sandwich plates that includes the kinematics of first-order shear-deformation theory as its baseline. The theory is variationally consistent and is derived from the virtual work principle. Novel piecewise-linear zigzag functions that provide a more realistic representation of the deformation states of transverse-shear-flexible plates than other similar theories are used. The formulation does not enforce full continuity of the transverse shear stresses across the plate's thickness, yet is robust. Transverse-shear correction factors are not required to yield accurate results. The theory is devoid of the shortcomings inherent in the previous zigzag theories including shear-force inconsistency and difficulties in simulating clamped boundary conditions, which have greatly limited the accuracy of these theories. This new theory requires only C^0-continuous kinematic approximations and is perfectly suited for developing computationally efficient finite elements. The theory should be useful for obtaining relatively efficient, accurate estimates of structural response needed to design high-performance load-bearing aerospace structures.

.

Nomenclature

a, b	lateral dimensions of a rectangular plate
$2h$	total plate (laminate) thickness
$2h^{(k)}$	thickness of the kth material layer (lamina)
(x_1, x_2)	reference plate-coordinate axes positioned in the middle plane of the laminate
z	thickness coordinate axis
N	number of material layers (laminae) through the laminate thickness
S_m	reference middle plane of the laminate
S_u, S_σ	parts of the cylindrical edge surface of the laminate where displacements and tractions are prescribed, respectively
C^0	denotes a continuous function whose first-order derivative is discontinuous

C_u, C_σ	intersections of the cylindrical edge surfaces (S_u, S_σ) with the middle surface S_m where displacements and traction resultants are prescribed, respectively
$\mathbf{s}, \mathbf{n}$	unit outward tangential and normal vectors to the mid-plane boundary (see Figure 1)
q	applied transverse pressure [force/length^2] (see Figure 1)
$(\overline{T}_1, \overline{T}_2, \overline{T}_z)$	prescribed in-plane and transverse shear tractions (see Eq. (14))
$(u_1^{(k)}, u_2^{(k)}, u_z)$	in-plane and transverse components of the displacement vector in the *k*th material layer (see Eqs. (1))
$(u, v, w, \theta_1, \theta_2, \psi_1, \psi_2)$	kinematic variables of the refined zigzag plate theory (see Eqs. (1))
(N_1, N_2, N_{12})	membrane stress resultants (see Eqs. (16))
(M_1, M_2, M_{12})	bending and twisting stress resultants (see Eqs. (17))
$(M_1^\phi, M_2^\phi, M_{12}^\phi, M_{21}^\phi)$	bending and twisting stress resultants due to zigzag kinematics (see Eqs. (17))
(Q_1, Q_2)	transverse shear stress resultants (see Eqs. (18))
(Q_1^ϕ, Q_2^ϕ)	transverse shear stress resultants due to zigzag kinematics (see Eqs. (18))
$\phi_\alpha^{(k)}$ $(\alpha = 1,2)$	zigzag functions (see Eqs. (1))
$\beta_\alpha^{(k)}$ $(\alpha = 1,2)$	derivatives of zigzag functions with respect to the thickness coordinate (see Eq. (2.2))
$\xi^{(k)}$	dimensionless thickness coordinates of the *k*th layer (lamina) (see Eq. (5))
$z_{(k)}$	thickness coordinate of the interface between the *k*th and $(k+1)$ th layers (see Figure 1)
$(u_{(k)}, v_{(k)})$	dimensionless in-plane displacements along the interface between the *k*th and $(k+1)$ th layers (see Figure 2)
$\left(\varepsilon_{11}^{(k)}, \varepsilon_{22}^{(k)}, \gamma_{12}^{(k)}, \gamma_{2z}^{(k)}, \gamma_{1z}^{(k)}\right)$	strains in the *k*th layer (see Eqs. (3))

$\gamma_\alpha(x_1,x_2)\ \ (\alpha=1,2)$	average shear strains (see Eq. (2.1) and Eq. (9))
$\eta_\alpha\ (\alpha=1,2)$	transverse-shear strain measures (see Eqs. (11))
$\psi_\alpha(x_1,x_2)\ \ (\alpha=1,2)$	zigzag amplitude functions (see Eqs. (1))
$\left(\sigma_{11}^{(k)},\sigma_{22}^{(k)},\tau_{12}^{(k)},\tau_{2z}^{(k)},\tau_{1z}^{(k)}\right)$	stresses in the *k*th layer (see Eqs. (3))
$E_i^{(k)}$	Young's moduli of the *k*th layer (see Table 1)
$G_{ij}^{(k)}$	shear moduli of the *k*th layer (see Table 1)
$\nu_{ij}^{(k)}$	Poisson ratios of the *k*th layer (see Table 1)
A_{ij}, B_{ij}, D_{ij}, and G_{ij}	constitutive stiffness coefficients (see Eqs. (22))
$C_{ij}^{(k)}, Q_{pq}^{(k)}$	in-plane and transverse shear elastic stiffness coefficients for the *k*th layer (see Eqs. (3))
$G_\alpha\quad(\alpha=1,2)$	weighted-average, laminate-dependent transverse shear constants (see Eqs. (12.3))
δ	variational operator (see eq. (14))
$\frac{\partial}{\partial x_\alpha}, (\bullet)_{,\alpha}$	partial differentiation
k^2	shear correction factor for First-order Shear Deformation Theory (FSDT)

1. Introduction

High-performance and lightweight characteristics of advanced composite materials have spurred a wider range of applicability of these materials in military and civilian aircraft, aerospace vehicles, and naval and civil structures. To realize the full potential of composite structures, further advances in structural design and analysis methods are necessary. In particular, development of cost-effective and reliable laminated-composite structures as the primary load-bearing components of a vehicle requires further advances in stress analysis and failure prediction methodologies.

A wide variety of modern civilian and military aircraft employ relatively thick laminated composites, with one hundred or more layers, in the primary load-bearing structures. Such structures can exhibit pronounced transverse shear deformation and, under certain conditions, design-critical thickness-stretch deformations. Fail-safe design of these structures requires accurate stress-analysis methods, particularly for regions of stress concentration. Computationally efficient analytical models based on beam, plate and shell assumptions that account for transverse shear and thickness-stretch deformations have recently been addressed in [1-3]. To achieve accurate computational models, three-dimensional finite element analyses are often preferred over beam, plate, and shell models that are based on First-order Shear-Deformation Theories (FSDT). This preference is because the latter tend to underestimate the normal stresses, particularly in highly heterogeneous and thick composite and sandwich laminates [4-7]. For composite laminates with hundreds of layers, however, three-dimensional modeling becomes prohibitively expensive, especially for nonlinear and progressive failure analyses. To realize improved response predictions based on beam, plate, and shell assumptions, a variety of refined theories have been developed, e.g., [8-11]. Many of these refined theories have significant flaws in their theoretical foundation and predictive capabilities and, for these reasons, have not found general acceptance in practical applications.

One class of refined theories that has emerged as practical for engineering applications is known as *zigzag* theories [12-24]. This class of theories employs a zigzag-like distribution for the in-plane displacements through the laminate thickness, while ensuring a fixed number of kinematic variables regardless of the number of material layers. It has been shown in [12-20] that zigzag theories provide sufficiently accurate response predictions for relatively thick laminated-composite and sandwich structures, including those for normal strains and stresses. Furthermore, these theories often yield the response predictions comparable to those that can be obtained from other layer-wise and higher-order theories that are more computationally intensive. To make a zigzag theory practical for a large-scale analysis and engineering design, the analytic framework of the theory must be well suited for an efficient finite element approximation.

Recently, Tessler et al. [25] elucidated several serious flaws in the most notable zigzag theories (see the discussion in Section 3), and proposed a *refined* zigzag methodology that eliminates these flaws in an original and theoretically consistent manner. This new methodology is general enough to provide a means for advancing this class of theories and is expected to be significantly more attractive for engineering practice, including applications of these theories in large-scale finite element analyses.

The aim of this report is to present a new zigzag theory for laminated-composite and sandwich plate structures that may exhibit a high degree of transverse shear flexibility, anisotropy, and heterogeneity. The range of applicability of the theory spans thin to relatively thick plates. This new theory is built upon the basic ideas of a refined zigzag theory for beams presented in [25]. Herein, FSDT is augmented with an improved zigzag kinematic field that involves a novel C^0-continuous (across lamina interfaces)

representation of the in-plane displacements. The kinematic field is independent of the number of material layers and does not require enforcement of transverse-shear-stress continuity to yield accurate results. Unlike other similar theories (e.g., [12,21]), the zigzag contribution to the in-plane displacement field is physically realistic, is zero-valued at the top and bottom plate surfaces, and accounts for the shear deformation of every lamina in a consistent way. As a result, transverse-shear correction factors are not needed. Additionally, the plate equilibrium equations, constitutive equations, boundary conditions, and strain-displacement relations are consistently derived from the virtual work principle.

One major benefit arising from the analytical form of this new theory is its ideal suitability to finite element modeling, where the kinematic-variable approximations need not exceed C^0 continuity. The implication of this attribute is that computationally efficient finite elements can be developed and used in general-purpose finite element codes. This benefit will enable an efficient use of accurate zigzag approximations in large-scale analyses to facilitate the development of robust designs of high-performance aerospace vehicles.

In the remainder of the paper, the theoretical foundation of the new theory and its quantitative assessment are detailed. The zigzag kinematic assumptions, strain-displacement equations, and constitutive lamina relations are presented in Section 2. The major theoretical anomalies associated with the previous zigzag theories are briefly discussed in Section 3. A set of unique zigzag functions is then introduced and their mathematical structure is described in Section 4. The plate equilibrium equations and their associated boundary conditions, derived from the virtual work principle, are presented in Section 5. In Section 6, an extensive quantitative assessment of the theory is carried out, using closed-form solutions for simply supported and cantilevered plates made of laminated-composite and sandwich material systems. Some of the example problems represent significant challenges for any approximate theory. It is demonstrated that this new zigzag theory eliminates a major flaw of other similar theories; that is, the theory enables accurate modeling of the clamped boundary condition while adhering strictly to the variationally required boundary conditions. Finally, several concluding remarks emphasizing the merits of the new theory are presented in Section 7.

2. Kinematics and formulation

Consider a laminated plate of uniform thickness $2h$ with N perfectly bonded orthotropic layers (or lamina) as shown in Figure 1. Points of the plate are located by the orthogonal Cartesian coordinates (x_1, x_2, z). The ordered pair $(x_1, x_2) \in S_m$ denotes the in-plane coordinates, where S_m represents the set of points given by the intersection of the plate with the plane $z = 0$, referred to herein as the middle reference plane (or midplane). The symbol $z \in [-h, h]$ is the through-the-thickness coordinate, with $z = 0$ identifying the midplane. The plate is subjected to a normal-pressure loading, $q(x_1, x_2)$, attributed to the midplane, S_m, that is defined as positive in the positive z direction. In addition, a traction vector, $\left(\overline{T}_1, \overline{T}_2, \overline{T}_z\right)$, is prescribed on $S_\sigma \subset S$, where S denotes the total cylindrical-edge surface. On the remaining part of the edge surface, $S_u \subset S$, displacement restraints are imposed (or prescribed). The sections of the plate edge are related by $S_\sigma \cup S_u = S$ and $S_\sigma \cap S_u = \varnothing$. Moreover, the curves $C_\sigma = S_\sigma \cap S_m$ and $C_u = S_u \cap S_m$ define the two parts of the total perimeter $C = C_\sigma \cup C_u$ surrounding the midplane region, S_m. Finally, it is presumed that the lamina constitutive properties may differ appreciably from lamina to lamina, the plate deformations result in small strains, and that body and

inertial forces are negligible.

The orthogonal components of the displacement vector, corresponding to material points of the plate (or laminate), are expressed as

$$
\begin{aligned}
u_1^{(k)}(x_1,x_2,z) &\equiv u(x_1,x_2) + z\,\theta_1(x_1,x_2) + \phi_1^{(k)}(z)\,\psi_1(x_1,x_2) \\
u_2^{(k)}(x_1,x_2,z) &\equiv v(x_1,x_2) + z\,\theta_2(x_1,x_2) + \phi_2^{(k)}(z)\,\psi_2(x_1,x_2) \\
u_z(x_1,x_2,z) &\equiv w(x_1,x_2)
\end{aligned}
\tag{1}
$$

where the in-plane displacement components $u_1^{(k)}$ and $u_2^{(k)}$ are comprised of constant, linear, and *zigzag* variations through the thickness. The zigzag variations are C^0 -continuous functions with discontinuous thickness-direction derivatives along the lamina interfaces. The superscript (k) is used to indicate quantities corresponding to the *k*th lamina, whereas the subscript (k) defines quantities corresponding to the interface between the *k* and (*k*+1) laminae. Thus, the *k*th lamina thickness is defined in the range $z \in [z_{(k-1)}, z_{(k)}]\,(k = 1,...,N)$ (see Figure 1). The transverse displacement u_z is assumed to be constant through the thickness and is independent of constitutive properties of the *k*th lamina; hence the superscript (k) does not appear in its definition.

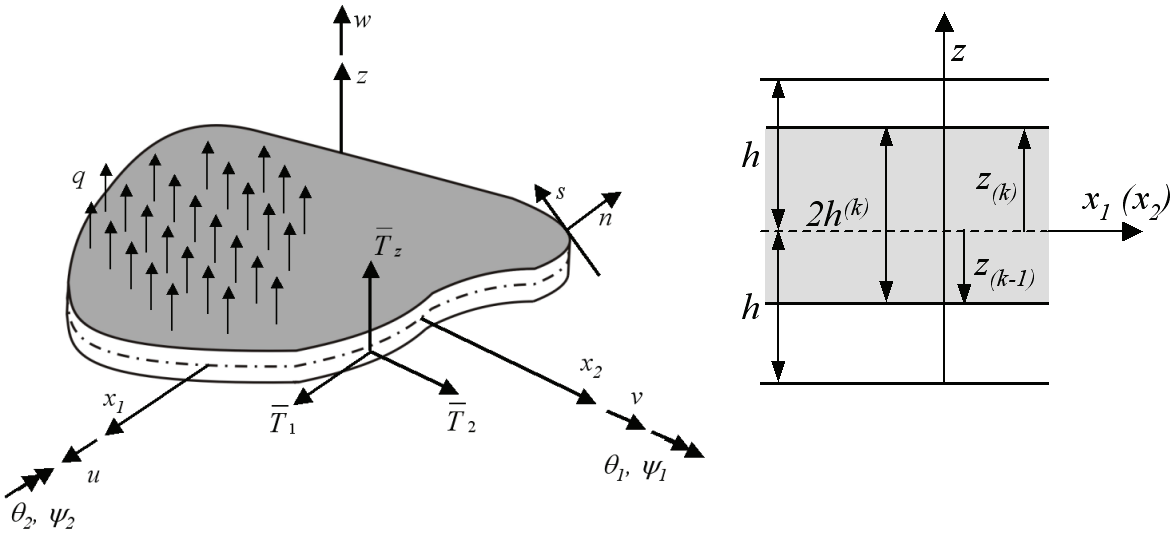

(a) (b)

Figure 1: (a) General plate notation, and (b) lamination notation.

The kinematic variables in Eqs. (1) can be interpreted as follows. For homogeneous plates, the zigzag functions $\phi_\alpha^{(k)}$ $(\alpha = 1,2)$ vanish identically and Eqs. (1) yield the kinematics of FSDT. For this degenerate case, u and v represent the midplane displacements along the coordinate directions x_1 and

x_2, respectively; θ_1 and θ_2 represent average bending rotations of the transverse normal about the positive x_2 and the negative x_1 directions, respectively; and w is the transverse deflection. For more precise definitions of the kinematic variables within FSDT refer, for example, to Ref. [1]. The symbols $\phi_\alpha^{(k)}$ $(\alpha = 1,2)$ denote through-the-thickness piecewise-linear zigzag functions associated with nonhomogeneous plates, yet to be defined. The $\psi_\alpha = \psi_\alpha(x_1, x_2)$ $(\alpha = 1,2)$ functions represent the spatial amplitudes of the zigzag displacements and, together with the other five kinematic variables, are the unknowns in the analysis. The *zigzag* displacements $\phi_\alpha^{(k)}\psi_\alpha$ $(\alpha = 1,2)$ may be regarded as corrections to the in-plane displacements associated with laminate heterogeneity.

Consistent with the kinematic assumptions in Eqs. (1), the theory accounts for transverse shear deformation. (Transverse normal deformations are neglected in the kinematics; however, their inclusion may be possible following, for example, [1]). Correspondingly, the in-plane and transverse shear strains are

$$\varepsilon_{11}^{(k)} = u_{,1} + z\theta_{1,1} + \phi_1^{(k)}\psi_{1,1} \tag{2.1}$$

$$\varepsilon_{22}^{(k)} = v_{,2} + z\theta_{2,2} + \phi_2^{(k)}\psi_{2,2} \tag{2.2}$$

$$\gamma_{12}^{(k)} = u_{,2} + v_{,1} + z(\theta_{1,2} + \theta_{2,1}) + \phi_1^{(k)}\psi_{1,2} + \phi_2^{(k)}\psi_{2,1} \tag{2.3}$$

$$\gamma_{\alpha z}^{(k)} = \gamma_\alpha + \beta_\alpha^{(k)}\psi_\alpha \quad (\alpha = 1,2) \tag{2.4}$$

where, henceforward, $(\bullet)_{,\alpha} \equiv \dfrac{\partial(\bullet)}{\partial x_\alpha}$ denotes a partial derivative with respect to the midplane coordinate, x_α $(\alpha = 1,2)$. Also, the following notation is introduced

$$\gamma_\alpha \equiv w_{,\alpha} + \theta_\alpha \quad (\alpha = 1,2) \tag{2.5}$$

$$\beta_\alpha^{(k)} \equiv \frac{\partial}{\partial z}\left(\phi_\alpha^{(k)}\right) \quad (\alpha = 1,2) \tag{2.6}$$

where the *shear angles* γ_α are uniform through the total laminate thickness, and $\beta_\alpha^{(k)}$ are piecewise constant functions that are uniform through the thickness of each individual lamina.

The generalized Hooke's law for the *k*th orthotropic lamina, whose principal material directions are arbitrary with respect to the midplane reference coordinates, $(x_1, x_2) \in S_m$, is written as

$$\begin{Bmatrix} \sigma_{11} \\ \sigma_{22} \\ \tau_{12} \\ \tau_{2z} \\ \tau_{1z} \end{Bmatrix}^{(k)} = \begin{bmatrix} C_{11} & C_{12} & C_{16} & 0 & 0 \\ C_{12} & C_{22} & C_{26} & 0 & 0 \\ C_{16} & C_{26} & C_{66} & 0 & 0 \\ 0 & 0 & 0 & Q_{22} & Q_{12} \\ 0 & 0 & 0 & Q_{12} & Q_{11} \end{bmatrix}^{(k)} \begin{Bmatrix} \varepsilon_{11} \\ \varepsilon_{22} \\ \gamma_{12} \\ \gamma_{2z} \\ \gamma_{1z} \end{Bmatrix}^{(k)} \tag{3}$$

where $C_{ij}^{(k)}$ $(i,j=1,2,6)$ and $Q_{pq}^{(k)}$ $(p,q=1,2)$ are the transformed elastic stiffness coefficients referred to the (x_1,x_2,z) coordinate system and relative to the plane-stress condition that ignores the transverse-normal stress. The expressions for these coefficients in terms of the elastic moduli corresponding to the material coordinates can be found, e.g., in [10].

3. Anomalies of previous zigzag theories

The 'linear zigzag model', that was developed for plate bending problems by Di Sciuva [12] and later examined further in [13-24], employs only five kinematic variables. In reference to Eqs. (1), these variables are u, v, w, ψ_1 and ψ_2. In contrast to Eqs. (1), Di Sciuva's zigzag-amplitude variables, ψ_1 and ψ_2, both contribute to the individual in-plane displacements, i.e., $u_1^{(k)} = f_1(u, w_{,1}, \psi_1, \psi_2)$ and $u_2^{(k)} = f_2(v, w_{,2}, \psi_1, \psi_2)$, thus resulting in a system of plate equilibrium equations that is coupled with respect to ψ_1 and ψ_2 (refer to Ref. [12] for the precise form of the displacement expansions of Di Sciuva's theory). Di Sciuva determines the appropriate zigzag functions by enforcing the transverse shear stresses to be continuous along the adjacent lamina interfaces and, in addition, by requiring that the zigzag functions vanish in a single layer that is selected a priori, labeled herein as a 'fixed layer.' As a result of the above stated assumptions and transverse shear stress-constraint conditions, Di Sciuva's theory attains the following characteristics: (a) the transverse shear stresses are uniform through the thickness and they correspond to those in the 'fixed layer'; (b) the laminate transverse shear stiffness is governed by the transverse shear moduli of the 'fixed layer' alone; (c) the transverse shear strains and stresses erroneously vanish along fully clamped edges; and (d) the integral of the transverse shear stress across the laminate thickness does not correspond to the shear force resultant obtained from the corresponding plate equilibrium equations – a physical inconsistency (or anomaly) in the definition of the shear force.

To remove the flaws associated with Di Sciuva's 'linear zigzag model', Tessler et al. [25] introduced a *refined* zigzag theory for laminated-composite and sandwich beams in which: (1) a novel zigzag function is used to produce non-vanishing zigzag displacements in every lamina, thus removing the shear stiffness bias associated with the 'fixed layer' approach, and (2) the equilibrium of transverse shear stresses along adjacent lamina interfaces is fulfilled only in an average sense. The resulting theory is devoid of the aforementioned flaws of the previous zigzag theories and has been shown to demonstrate consistently superior results. In what follows, an extension of the methodology presented in [25] to plates is described in detail.

4. Refined zigzag functions and transverse shear constitutive relations

The *refined zigzag functions* of the present theory are defined by using functions that are piecewise linear and C^0 continuous through the laminate thickness. For convenience, dimensionless lamina-interface displacements $u_{(i)}$ and $v_{(i)}$ $(i = 0,1,...,N)$ are used to define $\phi_1^{(k)}$ and $\phi_2^{(k)}$, respectively (see Figure 2 depicting the notation for a three-layered laminate).

Thus, for the kth lamina located in the range $[z_{(k-1)}, z_{(k)}]$, $\phi_1^{(k)}$ and $\phi_2^{(k)}$ are given as

$$\phi_1^{(k)} \equiv \tfrac{1}{2}(1-\xi^{(k)})\, u_{(k-1)} + \tfrac{1}{2}(1+\xi^{(k)})\, u_{(k)} \tag{4}$$

$$\phi_2^{(k)} \equiv \tfrac{1}{2}(1-\xi^{(k)})\, v_{(k-1)} + \tfrac{1}{2}(1+\xi^{(k)})\, v_{(k)}$$

where

$$\xi^{(k)} = [(z - z_{(k-1)})/h^{(k)} - 1] \in [-1,1] \quad (k = 1,...,N) \tag{5}$$

with the first lamina beginning at $z_{(0)} = -h$, the last (Nth) lamina ending at $z_{(N)} = h$, and the kth lamina ending at $z_{(k)} = z_{(k-1)} + 2h^{(k)}$, where $2h^{(k)}$ denotes the kth lamina thickness.

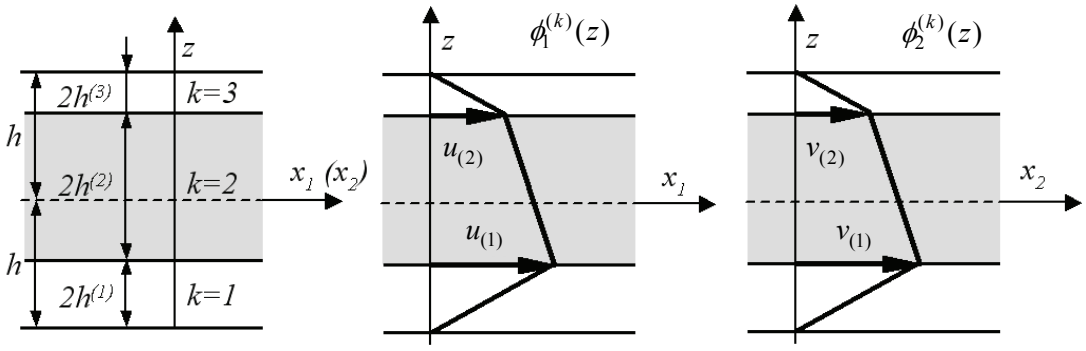

(a) Layer notation (b) Zigzag function $\phi_1^{(k)}$ (c) Zigzag function $\phi_2^{(k)}$

Figure 2. Notation for a three-layered laminate and $\phi_1^{(k)}$ and $\phi_2^{(k)}$ zigzag functions defined in terms of interfacial displacements, $u_{(i)}$ and $v_{(i)}$ $(i = 0,1,...,N)$.

Evaluating Eqs. (4) at the laminae interfaces gives rise to the definitions of the interfacial displacements

$$\begin{aligned} u_{(k-1)} &= \phi_1^{(k)}(\xi^{(k)} = -1), \quad u_{(k)} = \phi_1^{(k)}(\xi^{(k)} = 1) \\ v_{(k-1)} &= \phi_2^{(k)}(\xi^{(k)} = -1), \quad v_{(k)} = \phi_2^{(k)}(\xi^{(k)} = 1) \quad (k = 1,...,N) \end{aligned} \tag{6.1}$$

where the interfacial displacements at the bottom and top plate surfaces are set herein to vanish identically, i.e.

$$u_{(0)} = u_{(N)} = v_{(0)} = v_{(N)} = 0 \tag{6.2}$$

Substituting Eqs. (4) into Eqs. (2.6) results in the piecewise-constant functions $\beta_\alpha^{(k)}$ given by

$$\begin{Bmatrix} \beta_1^{(k)} \\ \beta_2^{(k)} \end{Bmatrix} = \frac{1}{2h^{(k)}} \begin{Bmatrix} u_{(k)} - u_{(k-1)} \\ v_{(k)} - v_{(k-1)} \end{Bmatrix} \tag{7}$$

Because the zigzag functions are zero-valued on the top and bottom surfaces, as defined by Eqs. (6), through-the-thickness integrals of the slope functions $\beta_\alpha^{(k)}$ $(\alpha = 1,2)$ vanish identically, i.e.

$$\int_{-h}^{h} \begin{Bmatrix} \beta_1^{(k)} \\ \beta_2^{(k)} \end{Bmatrix} dz = \begin{Bmatrix} \sum_{k=1}^{N} 2h^{(k)} \beta_1^{(k)} \\ \sum_{k=1}^{N} 2h^{(k)} \beta_2^{(k)} \end{Bmatrix} = \begin{Bmatrix} 0 \\ 0 \end{Bmatrix} \tag{8}$$

Integrating Eqs. (2.4) across the laminate thickness and normalizing the result by the total laminate thickness, reveals that

$$\begin{Bmatrix} \gamma_1 \\ \gamma_2 \end{Bmatrix} = \frac{1}{2h} \int_{-h}^{h} \begin{Bmatrix} \gamma_{1z}^{(k)} \\ \gamma_{2z}^{(k)} \end{Bmatrix} dz \tag{9}$$

Thus, γ_α $(\alpha = 1,2)$ represent the average transverse shear strains, coinciding with the common representation of the transverse shear strains used in FSDT. Also, Eqs. (9) indicate that the zigzag amplitude variables, ψ_α $(\alpha = 1,2)$, do not contribute to the average transverse shear strains.

The $u_{(k)}$ and $v_{(k)}$ interfacial displacements are obtained from Eqs. (7) in terms of $\beta_\alpha^{(k)}$ $(\alpha = 1,2; k = 1,...,N)$, i.e.

$$\begin{Bmatrix} u_{(k)} \\ v_{(k)} \end{Bmatrix} = 2h^{(k)} \begin{Bmatrix} \beta_1^{(k)} \\ \beta_2^{(k)} \end{Bmatrix} + \begin{Bmatrix} u_{(k-1)} \\ v_{(k-1)} \end{Bmatrix} \quad (k = 1,...,N) \tag{10.1}$$

or, alternatively,

$$\begin{Bmatrix} u_{(k)} \\ v_{(k)} \end{Bmatrix} = \begin{Bmatrix} \sum_{i=1}^{k} 2h^{(i)}\beta_1^{(i)} \\ \sum_{i=1}^{k} 2h^{(i)}\beta_2^{(i)} \end{Bmatrix} \quad (k = 1,...,N) \tag{10.2}$$

with Eqs. (6.2) defining zero-valued top- and bottom-surface interfacial displacements.

Following the approach in [25], the $\beta_\alpha^{(k)}$ functions are determined by first casting the transverse shear strains, Eqs. (2.4), in terms of the transverse-shear strain measures, $\eta_\alpha \equiv \gamma_\alpha - \psi_\alpha$ $(\alpha = 1,2)$, and the zigzag amplitude functions, ψ_α $(\alpha = 1,2)$, as

$$\begin{Bmatrix} \gamma_{1z} \\ \gamma_{2z} \end{Bmatrix}^{(k)} \equiv \begin{Bmatrix} \eta_1 \\ \eta_2 \end{Bmatrix} + \begin{bmatrix} (1+\beta_1^{(k)}) & 0 \\ 0 & (1+\beta_2^{(k)}) \end{bmatrix} \begin{Bmatrix} \psi_1 \\ \psi_2 \end{Bmatrix} \tag{11}$$

The η_α strain measures are set to vanish explicitly in Di Sciuva's theory [12] and enforced to vanish by way of penalty constraints in Averill's theory [21], thus equating γ_α to ψ_α. Presently, no such constraints are imposed on these strain measures.

The transverse shear stresses using Eqs. (3) and Eqs. (11) are given as

$$\begin{Bmatrix} \tau_{1z} \\ \tau_{2z} \end{Bmatrix}^{(k)} \equiv \begin{bmatrix} Q_{11} & Q_{12} \\ Q_{12} & Q_{22} \end{bmatrix}^{(k)} \left(\begin{Bmatrix} \eta_1 \\ \eta_2 \end{Bmatrix} + \begin{bmatrix} (1+\beta_1^{(k)}) & 0 \\ 0 & (1+\beta_2^{(k)}) \end{bmatrix} \begin{Bmatrix} \psi_1 \\ \psi_2 \end{Bmatrix} \right) \tag{12.1}$$

or, alternatively, they can be expressed as

$$\begin{Bmatrix} \tau_{1z} \\ \tau_{2z} \end{Bmatrix}^{(k)} \equiv \begin{bmatrix} Q_{11} & Q_{12} \\ Q_{12} & Q_{22} \end{bmatrix}^{(k)} \begin{Bmatrix} \eta_1 \\ \eta_2 \end{Bmatrix}$$

$$+ Q_{11}^{(k)}(1+\beta_1^{(k)}) \begin{Bmatrix} 1 \\ Q_{12}^{(k)}/Q_{11}^{(k)} \end{Bmatrix} \psi_1 + Q_{22}^{(k)}(1+\beta_2^{(k)}) \begin{Bmatrix} Q_{12}^{(k)}/Q_{22}^{(k)} \\ 1 \end{Bmatrix} \psi_2 \tag{12.2}$$

In this form of the transverse-shear constitutive relations, the stress vector associated with the η_α strain measures is independent of the zigzag functions. The second and third stress vectors include, as their normalization factors, the coefficients $Q_{\alpha\alpha}^{(k)}(1+\beta_\alpha^{(k)})$ $(\alpha = 1,2)$ that are dependent on the zigzag functions through $\beta_\alpha^{(k)}$. Herein, these normalization factors are set to be constant quantities, denoted as G_α $(\alpha = 1,2)$, thus imposing constraint conditions on the distribution of the zigzag functions.

These constraints give rise to the expressions for $\beta_\alpha^{(k)}$

$$\begin{Bmatrix} \beta_1^{(k)} \\ \beta_2^{(k)} \end{Bmatrix} = \begin{Bmatrix} \dfrac{G_1}{Q_{11}^{(k)}} - 1 \\ \dfrac{G_2}{Q_{22}^{(k)}} - 1 \end{Bmatrix} \tag{12.3}$$

The G_1 and G_2 constants are obtained by integrating Eqs. (12.3) through the laminate thickness while making use of Eqs. (8), resulting in

$$\begin{Bmatrix} G_1 \\ G_2 \end{Bmatrix} \equiv \begin{Bmatrix} \left(\dfrac{1}{2h} \displaystyle\int_{-h}^{h} \dfrac{dz}{Q_{11}^{(k)}} \right)^{-1} \\ \left(\dfrac{1}{2h} \displaystyle\int_{-h}^{h} \dfrac{dz}{Q_{22}^{(k)}} \right)^{-1} \end{Bmatrix} = \begin{Bmatrix} \left(\dfrac{1}{h} \displaystyle\sum_{k=1}^{N} \dfrac{h^{(k)}}{Q_{11}^{(k)}} \right)^{-1} \\ \left(\dfrac{1}{h} \displaystyle\sum_{k=1}^{N} \dfrac{h^{(k)}}{Q_{22}^{(k)}} \right)^{-1} \end{Bmatrix} \tag{12.4}$$

where it is seen that G_1 and G_2 are weighted-average transverse-shear stiffness coefficients of their respective lamina-level coefficients, $Q_{11}^{(k)}$ and $Q_{22}^{(k)}$.

Replacing Eqs. (12.3) into Eqs. (12.1), results in the transverse-shear constitutive relations of the form

$$\begin{Bmatrix} \tau_{1z} \\ \tau_{2z} \end{Bmatrix}^{(k)} = \begin{bmatrix} Q_{11} & Q_{12} \\ Q_{12} & Q_{22} \end{bmatrix}^{(k)} \begin{Bmatrix} \gamma_1 + \psi_1 \left(\dfrac{G_1}{Q_{11}^{(k)}} - 1 \right) \\ \gamma_2 + \psi_2 \left(\dfrac{G_2}{Q_{22}^{(k)}} - 1 \right) \end{Bmatrix} \tag{13.1}$$

where, with the use of Eqs. (12.4), the dimensionless stiffness ratios are given as

$$\frac{G_\alpha}{Q_{\alpha\alpha}^{(k)}} = \left(\frac{Q_{\alpha\alpha}^{(k)}}{2h} \int_{-h}^{h} \frac{dz}{Q_{\alpha\alpha}^{(k)}} \right)^{-1} \quad (\alpha = 1, 2) \tag{13.2}$$

These ratios are, in general, piecewise-constant through the laminate thickness; however, for homogeneous plates, they are unit-valued. Thus, for homogeneous plates, the zigzag transverse-shear contributions vanish, in which case Eqs. (13.1) become identical to the corresponding relations of FSDT.

The $\phi_\alpha^{(k)}$ $(\alpha = 1,2)$ zigzag functions are determined by substituting Eqs. (10.2) and Eqs. (12.3) into Eqs. (4), while making use of Eqs. (5), resulting in

$$\phi_\alpha^{(1)} = (z+h)\left(\frac{G_\alpha}{Q_{\alpha\alpha}^{(1)}} - 1\right) \quad (k=1)$$

$$\phi_\alpha^{(k)} = (z+h)\left(\frac{G_\alpha}{Q_{\alpha\alpha}^{(k)}} - 1\right) + \sum_{i=2}^{k} 2h^{(i-1)}\left(\frac{G_\alpha}{Q_{\alpha\alpha}^{(i-1)}} - \frac{G_\alpha}{Q_{\alpha\alpha}^{(k)}}\right) \quad (k=2,...,N) \tag{13.3}$$

$$z \in [z_{(k-1)}, z_{(k)}]; \; z_{(0)} = -h; \; z_{(k)} = z_{(k-1)} + 2h^{(k)} \quad (k=1,...,N; \; \alpha = 1,2)$$

It is seen that the zigzag functions are independent of the state of deformation and are represented by C^0-continuous, piecewise linear functions of the thickness coordinate. These functions possess slope discontinuity along lamina interfaces and vary linearly through the thickness of each lamina. Within each lamina, the transverse shear properties are represented by the stiffness ratios defined in Eqs. (13.2). For homogeneous plates, the zigzag functions vanish identically.

The zigzag amplitudes, ψ_α $(\alpha = 1,2)$, are vector functions of the actual response due to the applied loading, and they provide the proper scaling of the zigzag functions, thus controlling the total zigzag contribution to the in-plane displacements. The two zigzag amplitude functions and the remaining five kinematic variables constitute a set of seven kinematic variables associated with this refined zigzag plate theory.

5. Equilibrium equations, boundary conditions, and constitutive relations

The plate equilibrium equations and boundary conditions are derived from the virtual work principle which, neglecting body forces and assuming zero shear tractions on the top and bottom bounding plate surfaces, may be written as

$$\begin{aligned} 0 = &\int_{S_m}\int_{-h}^{h}\left(\sigma_{11}^{(k)}\delta\varepsilon_{11}^{(k)} + \sigma_{22}^{(k)}\delta\varepsilon_{22}^{(k)} + \tau_{12}^{(k)}\delta\gamma_{12}^{(k)} + \tau_{1z}^{(k)}\delta\gamma_{1z}^{(k)} + \tau_{2z}^{(k)}\delta\gamma_{2z}^{(k)}\right)dz\,dS \\ &- \int_{S_m}\left(q\,\delta w\right)dS - \int_{C_\sigma}\int_{-h}^{h}\left[\overline{T}_1\delta u_1^{(k)} + \overline{T}_2\delta u_2^{(k)} + \overline{T}_z\delta u_z^{(k)}\right]ds\,dz \end{aligned} \tag{14}$$

where δ is the variational operator; all other symbols have been defined in Section 2.

Substituting Eqs. (1) and (2) into Eq. (14), and integrating across the plate thickness yields the two-dimensional statement of virtual work

$$
\begin{aligned}
0 = & \int_{S_m} [N_1 \delta u_{,1} + N_2 \delta v_{,2} + N_{12}(\delta u_{,2} + \delta v_{,1}) \\
& + M_1 \delta \theta_{1,1} + M_2 \delta \theta_{2,2} + M_{12}(\delta \theta_{1,2} + \delta \theta_{2,1}) \\
& + Q_1(\delta w_{,1} + \delta \theta_1) + Q_2(\delta w_{,2} + \delta \theta_2) - q \delta w] dS \\
& - \int_{C_\sigma} [\bar{N}_{1n} \delta u + \bar{N}_{2n} \delta v + \bar{Q}_{zn} \delta w + \bar{M}_{1n} \delta \theta_y + \bar{M}_{2n} \delta \theta_x] ds \\
& + \int_{S_m} [M_1^\phi \delta \psi_{1,1} + M_2^\phi \delta \psi_{2,2} + M_{12}^\phi \delta \psi_{1,2} + M_{21}^\phi \delta \psi_{2,1} + Q_1^\phi \delta \psi_1 + Q_2^\phi \delta \psi_2] dS \\
& - \int_{C_\sigma} [\bar{M}_{1n}^\phi \delta \psi_1 + \bar{M}_{2n}^\phi \delta \psi_2] ds
\end{aligned}
\tag{15}
$$

where the last two lines correspond to the zigzag kinematics contributions. In Eq. (15), the membrane stress resultants and conjugate strain measures are

$$
\mathbf{N}_m^T \equiv \left\{ N_1, N_2, N_{12} \right\} = \int_{-h}^{h} \left\{ \sigma_{11}^{(k)}, \sigma_{22}^{(k)}, \tau_{12}^{(k)} \right\} dz \tag{16.1}
$$

$$
\mathbf{e}_m^T \equiv \left\{ u_{,1}, \; v_{,2}, \; u_{,2} + v_{,1} \right\} \tag{16.2}
$$

Likewise, the bending stress resultants and conjugate strain measures are

$$
\begin{aligned}
\mathbf{M}_b^T & \equiv \left\{ M_1, M_1^\phi, M_2, M_2^\phi, M_{12}, M_{12}^\phi, M_{21}^\phi \right\} \\
& = \int_{-h}^{h} \left\{ z \sigma_{11}^{(k)}, \phi_1^{(k)} \sigma_{11}^{(k)}, z \sigma_{22}^{(k)}, \phi_2^{(k)} \sigma_{22}^{(k)}, z \tau_{12}^{(k)}, \phi_1^{(k)} \tau_{12}^{(k)}, \phi_2^{(k)} \tau_{12}^{(k)} \right\} dz
\end{aligned}
\tag{17.1}
$$

$$
\mathbf{e}_b^T \equiv \left\{ \theta_{1,1}, \psi_{1,1}, \theta_{2,2}, \psi_{2,2}, \theta_{1,2} + \theta_{2,1}, \psi_{1,2}, \psi_{2,1} \right\} \tag{17.2}
$$

and the transverse shear stress resultants and conjugate strain measures are

$$
\mathbf{Q}_s^T \equiv \left\{ Q_2, Q_2^\phi, Q_1, Q_1^\phi \right\} = \int_{-h}^{h} \left\{ \tau_{2z}^{(k)}, \beta_2^{(k)} \tau_{2z}^{(k)}, \tau_{1z}^{(k)}, \beta_1^{(k)} \tau_{1z}^{(k)} \right\} dz \tag{18.1}
$$

$$
\mathbf{e}_s^T \equiv \left\{ w_{,2} + \theta_2, \psi_2, w_{,1} + \theta_1, \psi_1 \right\} \tag{18.2}
$$

The force and moment resultants due to the prescribed tractions have the form

$$
\begin{aligned}
& \left\{ \bar{N}_{1n}, \bar{N}_{2n}, \bar{Q}_{zn}, \bar{M}_{1n}, \bar{M}_{2n}, \bar{M}_{1n}^\phi, \bar{M}_{2n}^\phi \right\} \\
& = \int_{-h}^{h} \left\{ \bar{T}_1, \bar{T}_2, \bar{T}_z, z \bar{T}_1, z \bar{T}_2, \phi_1^{(k)} \bar{T}_1, \phi_2^{(k)} \bar{T}_2 \right\} dz
\end{aligned}
\tag{19}
$$

Integrating Eq. (15) by parts results in seven equilibrium equations and associated boundary conditions. The equilibrium equations are

$$\begin{aligned}
\delta u &: \quad N_{1,1} + N_{12,2} = 0 \\
\delta v &: \quad N_{12,1} + N_{2,2} = 0 \\
\delta w &: \quad Q_{1,1} + Q_{2,2} + q = 0 \\
\delta \theta_1 &: \quad M_{1,1} + M_{12,2} - Q_1 = 0 \\
\delta \theta_2 &: \quad M_{12,1} + M_{2,2} - Q_2 = 0 \\
\delta \psi_1 &: \quad M^{\phi}_{1,1} + M^{\phi}_{12,2} - Q^{\phi}_1 = 0 \\
\delta \psi_2 &: \quad M^{\phi}_{21,1} + M^{\phi}_{2,2} - Q^{\phi}_2 = 0
\end{aligned} \tag{20}$$

The kinematic and force boundary conditions are given by

$$u = \overline{u} \text{ on } C_u \text{ or } N_1 n_1 + N_{12} n_2 = \overline{N}_{1n} \text{ on } C_\sigma \tag{21.1}$$

$$v = \overline{v} \text{ on } C_u \text{ or } N_{12} n_1 + N_2 n_2 = \overline{N}_{2n} \text{ on } C_\sigma \tag{21.2}$$

$$w = \overline{w} \text{ on } C_u \text{ or } Q_1 n_1 + Q_2 n_2 = \overline{Q}_{zn} \text{ on } C_\sigma \tag{21.3}$$

$$\theta_1 = \overline{\theta}_1 \text{ on } C_u \text{ or } M_1 n_1 + M_{12} n_2 = \overline{M}_{1n} \text{ on } C_\sigma \tag{21.4}$$

$$\theta_2 = \overline{\theta}_2 \text{ on } C_u \text{ or } M_{12} n_1 + M_2 n_2 = \overline{M}_{2n} \text{ on } C_\sigma \tag{21.5}$$

$$\psi_1 = \overline{\psi}_1 \text{ on } C_u \text{ or } M^{\phi}_1 n_1 + M^{\phi}_{12} n_2 = \overline{M}^{\phi}_{1n} \text{ on } C_\sigma \tag{21.6}$$

$$\psi_2 = \overline{\psi}_2 \text{ on } C_u \text{ or } M^{\phi}_{21} n_1 + M^{\phi}_2 n_2 = \overline{M}^{\phi}_{2n} \text{ on } C_\sigma \tag{21.7}$$

where $n_1 = \cos(x_1, n)$ and $n_2 = \cos(x_2, n)$ are the components (direction cosines) of the unit outward normal vector to the cylindrical plate edges.

The plate constitutive relations are derived by using Eqs. (2) and (3) with Eqs. (16)-(18), and integrating over the laminate thickness. The resulting constitutive relations of the new zigzag plate theory are expressed in matrix form as

$$\begin{Bmatrix} \mathbf{N}_m \\ \mathbf{M}_b \\ \mathbf{Q}_s \end{Bmatrix} = \begin{bmatrix} \mathbf{A} & \mathbf{B} & \mathbf{0} \\ \mathbf{B}^T & \mathbf{D} & \mathbf{0} \\ \mathbf{0} & \mathbf{0} & \mathbf{G} \end{bmatrix} \begin{Bmatrix} \mathbf{e}_m \\ \mathbf{e}_b \\ \mathbf{e}_s \end{Bmatrix} \tag{22}$$

where expressions for the components of the stiffness matrices $\mathbf{A} \equiv [A_{ij}] \quad (i,j = 1-3)$, $\mathbf{B} \equiv [B_{ij}]\,(i = 1-3; j = 1-7)$, $\mathbf{D} \equiv [D_{ij}]\,(i,j = 1-7)$, and $\mathbf{G} \equiv [G_{ij}] \quad (i,j = 1-4)$ are given in Appendix A.

Introducing Eqs. (22) into Eqs. (20) results in seven partial differential equilibrium equations in terms of seven kinematic variables, resulting in a 14th-order theory. The equilibrium equations can be solved exactly or approximately depending on the complexity of the material lay-up, boundary conditions, and loading. In addition, because the highest partial derivative appearing in the strain measures in Eqs. (15) are first order, computationally efficient C^0-continuous plate finite elements can be developed, thus enabling application of this zigzag theory in large-scale analyses of complex aerospace structures.

6. Example problems and results

To determine the accuracy of the present zigzag plate theory, analytic solutions for simply supported and cantilevered rectangular laminates are derived and detailed distributions of the displacements and stresses are examined. The rectangular laminates are defined on the domain $x_1 \in [0,a],\, x_2 \in [0,b],\, z \in [-h,h]$.

Example 1: A simply supported rectangular plate is subjected to the sinusoidal transverse pressure $q(x_1,x_2) = q_o \sin(\pi x_1/a)\sin(\pi x_2/b)$. The simply supported boundary conditions are obtained from Eqs. (21). For cross-ply and uniaxial laminates, the kinematic and force boundary conditions along $x_1 \in [0,a]$ are

$$v = w = \theta_2 = \psi_2 = 0 \tag{23.1}$$

$$N_1 = M_1 = M_1^{\phi} = 0 \tag{23.2}$$

and along $x_2 \in [0,b]$,

$$u = w = \theta_1 = \psi_1 = 0 \tag{23.3}$$

$$N_2 = M_2 = M_2^{\phi} = 0 \tag{23.4}$$

For this set of boundary conditions, the exact solutions are obtained by the following trigonometric expansions

$$w = W \sin(\pi x_1/a)\sin(\pi x_2/b) \tag{24.1}$$

$$\begin{Bmatrix} u \\ \theta_1 \\ \psi_1 \end{Bmatrix} = \begin{Bmatrix} U \\ \Theta_1 \\ \Psi_1 \end{Bmatrix} \cos(\pi x_1/a)\sin(\pi x_2/b) \tag{24.2}$$

$$\begin{Bmatrix} v \\ \theta_2 \\ \psi_2 \end{Bmatrix} = \begin{Bmatrix} V \\ \Theta_2 \\ \Psi_2 \end{Bmatrix} \sin(\pi x_1 / a)\cos(\pi x_2 / b) \tag{24.3}$$

where $\{U, V, W, \Theta_1, \Theta_2, \Psi_1, \Psi_2\}$ are the unknown magnitudes of the kinematic variables that are determined from satisfaction of the equilibrium equations.

For antisymmetric angle-ply laminates, the kinematic and force boundary conditions along $x_1 \in [0, a]$ are

$$u = w = \theta_2 = \psi_2 = 0 \tag{25.1}$$

$$N_{12} = M_1 = M_1^{\phi} = 0 \tag{25.2}$$

and along $x_2 \in [0, b]$

$$v = w = \theta_1 = \psi_1 = 0 \tag{25.3}$$

$$N_{12} = M_2 = M_2^{\phi} = 0 \tag{25.4}$$

Thus, the trigonometric expansions that satisfy Eqs. (25) exactly differ from those in Eq. (24) only for the *u* and *v* variables, and they are given by

$$u = U \sin(\pi x_1 / a)\cos(\pi x_2 / b), \;\; v = V \cos(\pi x_1 / a)\sin(\pi x_2 / b) \tag{26}$$

Example 2: A cantilevered rectangular plate clamped along a single edge $(x_1 = 0)$, free along the other edges, and subjected to the uniform transverse pressure $q(x_1, x_2) = q_o$. The clamped boundary conditions along $x_1 = 0$ are

$$u = v = w = \theta_1 = \theta_2 = \psi_1 = \psi_2 = 0 \tag{27.1}$$

Unlike the previous zigzag theories where the clamped boundary conditions result in erroneous solutions for transverse shear stresses and forces that vanish along the clamped edges, the solutions of the present theory do not possess such anomalies. For instance, along the clamped boundary at $x_1 = 0$, the kinematic constraints in Eqs. (27.1), with the use of Eqs. (2.5), (13.2), and (18), give rise to the following transverse-shear stresses, $\tau_{1z}^{(k)}(0, x_2, z)$, and force, $Q_1(0, x_2)$:

$$\begin{Bmatrix} \tau_{1z}^{(k)} \\ Q_1 \end{Bmatrix}_{(x_1=0)} = \begin{Bmatrix} Q_{11}^{(k)} \\ \int_{-h}^{h} Q_{11}^{(k)} dz \end{Bmatrix} w_{,1}(0, x_2) \tag{27.2}$$

where, in general, $w_{,1}(0, x_2) \neq 0$.

The traction-free boundary conditions along the edge $x_1 = a$ are

$$N_1 = N_{12} = M_1 = M_{12} = Q_1 = M_1^{\phi} = M_{12}^{\phi} = 0 \tag{28.1}$$

and along the edge $x_2 \in [0, b]$

$$N_{12} = N_2 = M_{12} = M_2 = Q_2 = M_{12}^{\phi} = M_2^{\phi} = 0 \tag{28.2}$$

For both example problems, various laminates are considered with the emphasis on relatively thick laminated composite and sandwich plates having the span-to-thickness ratio $a/2h = b/2h = 5$. The mechanical material properties are listed in Table 1, whereas in Table 2 the stacking sequences of the laminates are summarized.

The example problems include: (1) a two-layer, cross-ply carbon-epoxy laminate, labeled as laminate A; (2) three variations of a three-layer sandwich laminate, laminates B, B_1, and B_2, having uniaxial carbon-epoxy face sheets and a thick, closed-cell polyvinyl chloride (PVC) core. Herein, PVC is represented as an isotropic material. Laminates B_1, and B_2 have progressively thinner face sheets; (3) a sandwich laminate with two-layered titanium face sheets and a thick titanium honeycomb core, laminate F; and (4) a five-layer, angle-ply sandwich laminate with carbon-epoxy face sheets and a thick PVC core, laminate G.

For comparison purposes, additional analytic and finite element solutions were also obtained for the corresponding boundary-value problems using the three-dimensional elasticity theory [27, 28], FSDT, Di Sciuva theory [12], and MSC/MD-NASTRAN finite element code [29]. Note that application of FSDT generally requires the use of shear correction factors. For laminated composites, lamination-dependent shear correction factors have been shown to provide relatively accurate deflection predictions (e.g., refer to [30, 31]). Yet, such shear corrections fail to furnish substantial improvements for the normal strain and stress predictions. Presently, to establish a common framework reference for FSDT, $k^2 = 5/6$, a shear correction factor that is appropriate for homogeneous plates, was used throughout.

For the simply supported cross-ply and uniaxial laminates, the exact solutions for the FSDT and Di Sciuva zigzag theory were obtained using the trigonometric functions in Eqs. (25.3) (excluding those functions for ψ_α $(\alpha = 1, 2)$ which do not appear in FSDT). For the angle-ply antisymmetric laminates, Di Sciuva theory permits only approximate solutions to be determined. Presently, the Rayleigh-Ritz method was employed, where the kinematic variables were approximated with suitable Gram-Schmidt polynomials [26] that satisfy the kinematic boundary conditions exactly, Eqs. (26.1) and (26.2) (refer to Appendix B for details on the Gram-Schmidt polynomials). Furthermore, for the simply supported cross-ply and angle-ply antisymmetric laminates, exact three-dimensional elasticity solutions were obtained using the solution procedures developed by Pagano [27] and Burton and Noor [28].

For the cantilevered laminates, approximate solutions corresponding to Di Sciuva and refined (present) zigzag theories were developed using the Rayleigh-Ritz method. Here the displacement approximations are based on the Gram-Schmidt polynomials, using seven functions along the x_1 axis and five along the x_2 axis (see Appendix B). Furthermore, for the cantilevered plate (laminate B), a high-fidelity three-dimensional (3D) finite element solution was obtained by using MSC/MD-NASTRAN. The model is regularly discretized and is comprised of three elements through the thickness for each face

sheet, six elements through the core thickness, and sixty subdivisions along each span direction, with the total of 43,200 HEXA20, linear-strain elements.

The numerical and graphical results that follow are labeled as:

- 3D Elasticity (three-dimensional elasticity solutions using procedures developed by Pagano [27] for cross-ply laminates and by Noor and Burton [28] for angle-ply antisymmetric laminates).
- FSDT (First-order Shear Deformation Theory, $k^2 = 5/6$).
- Zigzag (D) (Di Sciuva [12]).
- Zigzag (R) (present, refined zigzag theory).
- 3D FEM (three-dimensional FEM solution using MSC/MD-NASTRAN [29]).
- Zigzag (R-E) (transverse shear stresses obtained by way of integrating three-dimensional elasticity equilibrium equations, using the normal and in-plane shear stresses derived from the refined zigzag theory).

Comparisons of the maximum deflection and maximum top-surface displacement are presented for the simply supported square laminates ($a/2h = b/2h = 5$) in Tables 3 and 4. These results demonstrate that both zigzag theories predict accurate plate displacements as compared to the three-dimensional elasticity solution, with the refined theory achieving slightly more accurate predictions. The laminate G case is somewhat pathological for Zigzag (D), because the solution in this case is only approximate and has not converged. The deflections predicted by FSDT are generally overly stiff; however, they are expected to improve substantially with the use of lamination-dependent shear correction factors. In Table 5, the range of applicability of the various theories is examined by comparing the maximum (central) plate deflection for a simply supported sandwich laminate B, where the solutions correspond to the span-to-thickness ratio in the range of 4 through 200. These results are also plotted in Figures 3(a) and 3(b). It is observed that both zigzag theories predict accurate deflections for all span-to-thickness ratios examined, whereas FSDT is overly stiff, especially in the thick regime, as expected. Even for a relatively thin laminate B ($a/2h = 50$), FSDT underestimates the maximum deflection by about 36%, which means that a much more significant shear correction factor would be required for FSDT for this type of laminate.

For the simply supported laminates, normalized through-the-thickness distributions for the in-plane displacement, $\bar{u}_1 = (10^4 D_{11}/q_o a^4)\, u_1^{(k)}(0, a/2, z)$, the normal stress, $\bar{\sigma}_{11} \equiv \left((2h)^2/q_0 a^2\right) \times \sigma_{11}^{(k)}(a/2, a/2, z)$, and the transverse-shear stress, $\bar{\tau}_{1z} \equiv (2h/q_0 a)\tau_{1z}^{(k)}(0, a/2, z)$, are depicted in Figures 4-21.

For laminate A – an asymmetric cross-ply carbon-epoxy composite – the $\bar{u}_1$ and $\bar{\sigma}_{11}$ quantities are accurately modeled by the FSDT, Zigzag (D), and Zigzag (R) theories, with Zigzag (D) producing slightly underestimated $\bar{u}_1$ displacement near the top surface (Figures 4-6). The major result differences for this laminate correspond to the $\bar{\tau}_{1z}$ distribution (Figure 6), where both FSDT and Zigzag (R) produce piecewise constant stresses, whereas Zigzag (D) gives a uniform (constant) distribution for $\bar{\tau}_{1z}$ that is significantly less accurate than the predictions of the other two theories. In addition, Zigzag (R) theory provides a more accurate evaluation of the average transverse shear stress within each lamina than does

FSDT. Also, the $\overline{\tau}_{1z}$ stress, obtained by equilibrium-based method, Zigzag (R-E), is best correlated with the three-dimensional elasticity solution (3D Elasticity).

The $\overline{u}_1$, $\overline{\sigma}_{11}$, and $\overline{\tau}_{1z}$ results for sandwich panels B, B_1 and B_2 that have constant-thickness carbon-epoxy face sheets and a PVC core are provided in Figures 7-15. The three laminates differ in terms of the face sheet thicknesses, starting with the thickest face sheets in laminate B and progressing to thinner face sheets in laminates B_1 and B_2. This study evaluates the effect of face sheet thinness on the through-the-thickness displacement and stress variations. As evidenced from Figure 7, the $\overline{u}_1$ zigzag effect is very strong in laminate B, and is less pronounced as the face-sheet thickness diminishes, as shown Figures 10 and 13 for laminates B_1 and B_2, respectively. For laminate B, the top- and bottom-surface values of the $\overline{u}_1$ displacement are significantly underestimated by FSDT that is only capable of a linear (average) distribution. Also, as shown in Figure 8, FSDT grossly underestimates the normal stress $\overline{\sigma}_{11}$ on the bounding surfaces where the greatest compression and tension occur. As the face sheets become thinner in relation to the core thickness, the FSDT predictions for $\overline{u}_1$ and $\overline{\sigma}_{11}$ tend to improve, as evidenced from Figures 7, 8, 10, 11, 13, and 14. However, FSDT tends to overestimate the transverse shear stress, $\overline{\tau}_{1z}$, significantly, while underestimating this stress in the core (refer to Figures 9, 12, and 15). As seen from Figures 9, 12, and 15, Zigzag (D) provides accurate response predictions for all three sandwich panels, with the exception of the transverse shear stress; the $\overline{\tau}_{1z}$ distributions are accurate within the core but erroneous in the face sheets. By contrast, Zigzag (R) yields accurate solutions of all response quantities for the three sandwich panels examined. When the transverse shear stresses are evaluated from the constitutive relations, the theory provides the correct average values in the face sheets and in the core. Moreover, the equilibrium-based method, Zigzag (R-E), furnishes the superior transverse shear stresses that are virtually indistinguishable from those of three-dimensional elasticity.

The sandwich study just presented illuminates some of the basic flaws in the classical sandwich-modeling assumptions, i.e., in-plane displacements are linear through-the-thickness and normal stresses are negligible in the core, and in-plane displacements are constant and transverse-shear stresses are negligible in the face sheets (e.g., refer to [32-34]). The hypothesis concerning the normal stresses is generally correct in the range of face-sheet thicknesses examined, as seen in Figures 8, 11, and 14; whereas the assumptions concerning the in-plane displacements and the transverse shear stresses are only confirmed for the sandwich panels with very thin face sheets. As seen in Figure 7, which depicts the laminate B results, the in-plane displacement exhibits a high gradient through the face sheets, thus departing appreciably from the classical, membrane assumption of uniform displacement. Furthermore, the average transverse shear stress in the face sheets is higher than in the core (see Figure 9), again contrasting with the classical assumption of negligible transverse shear stress in the face sheets.

The displacement and stress results for laminate F – a cross-ply sandwich with a lower degree of anisotropy than laminate B – are depicted in Figures 16–18. For this laminate, the zigzag effect of the in-plane displacement is somewhat less pronounced than for laminate B. As in the previous example, Zigzag (R) yields highly accurate predictions of all response quantities. It is seen that FSDT provides over estimated values for the in-plane displacement on the bounding surfaces. Also, it is evident from Figure 18(a) that the integral of the shear stress over the thickness computed using the Zigzag (D) transverse shear stress would result in a significantly greater value than the exact shear force.

Figures 19–21 demonstrate the results for laminate G – an angle-ply antisymmetric sandwich plate with multilayered face sheets. This is a highly challenging test case for any lamination theory. For this lamination, only an approximate solution can be obtained for Zigzag (D), requiring a large number of

suitable shape functions to achieve a converged solution. Using the Rayleigh-Ritz method with the Gram-Schmidt polynomials approximating the kinematic variables (see the details of the approximating functions in Appendix B), a relatively inaccurate solution was obtained. Consequently, the Zigzag (D) results for the in-plane displacement (Figure 19) and normal stress (Figure 20) are somewhat erroneous. On the other hand, Zigzag (R) enables an exact solution to be obtained for this problem, once again yielding highly accurate predictions of the response quantities. As in the previous examples, FSDT models the in-plane displacement response only in an average sense (a linear distribution through the thickness), leading to a significant underestimation (a non conservative prediction) of the normal stress in the face sheets.

To examine the effect of clamped boundary conditions, a square cantilevered laminate B under a uniform transverse pressure was examined. Table 6 summarizes the maximum deflection calculated using the three different theories and a three-dimensional finite element solution that serves as a reference. The FSDT deflection is underestimated by an order of magnitude. The two zigzag theories give accurate results, with Zigzag (R) producing a somewhat superior deflection prediction.

For the cantilevered sandwich laminate B, normalized through-the-thickness distributions of the in-plane displacement, $\bar{u}_1 = (10^4 D_{11}/q_o a^4)\, u_1^{(k)}(a, a/2, z)$, the normal stress, $\bar{\sigma}_{11} = \left((2h)^2/q_0 a^2\right)\times \sigma_{11}^{(k)}(a/5, a/2, z)$, and the transverse-shear stress, $\bar{\tau}_{1z} = \left(2h/q_0 a\right)\times\ \tau_{1z}^{(k)}(a/5, a/2, z)$, are provided in Figures 22–24. The stresses were computed near the clamped edge $(x_1 = a/5, x_2 = a/2)$ to allow for proper comparisons with the accurate stresses obtained from the 3D FEM analysis. For this problem, both zigzag theories produce accurate results; however, application of Zigzag (R) resulted in superior predictions of transverse shear stresses. Finally, the normalized transverse shear force, $\bar{Q}_1 = \dfrac{1}{q_0 a}\int_{-h}^{h} \tau_{1z}^{(k)}\, dz$, evaluated at $x_2 = a/2$, is plotted versus the normalized axial coordinate, x_1/a, as shown in Figure 25. For this problem, both FSDT and Zigzag (R) predict the correct linear distribution, yielding a maximum value at the clamped edge and vanishing at the free edge. This contrasts with an erroneous Zigzag (D) solution that varies in a non-linear manner across the span and which vanishes at the clamped edge.

7. Conclusions

A refined zigzag theory has been developed for laminated-composite and sandwich plates that exhibit a high degree of transverse shear flexibility, anisotropy, and heterogeneity. In this refined theory, a first-order shear-deformation theory is used as a baseline for the kinematic assumptions with a set of novel piecewise-continuous zigzag displacements added to the in-plane displacement components. The resulting kinematic field is independent of the number of material layers, and the zigzag displacements are defined by requiring only partial lamina-interface continuity requirements of transverse shear stresses. The force equilibrium equations, boundary conditions, and strain-displacement relations are completely consistent with respect to the virtual work principle, and transverse-shear correction factors are not required. The refined zigzag theory is better suited for engineering practice than previous similar theories because of its relative simplicity and its ability to model accurately the transverse shear and in-plane deformations of the individual laminae in a physically realistic manner. Unlike other similar theories, meaningful in-plane and transverse shear stresses are obtained directly from the constitutive equations, in a theoretically consistent

manner. The new theory is devoid of a major shortcoming of other similar theories; that is, the new theory enables accurate modeling of clamped boundary conditions.

Results for several example problems have been presented that highlight the superior predictive capability attainable with the present theory and its ability to model correctly clamped boundary conditions. The critical quantitative assessment of the new theory, that included analyses of highly heterogeneous sandwich laminates in bending, revealed that this refined zigzag theory is more accurate than previous similar theories.

An additional and important benefit is that the new zigzag theory lends itself well for finite element approximations. In particular, the theory is perfectly suited for the development of computationally efficient, C^0-continuous finite elements. Because of a wide applicability range that includes laminated-composite and sandwich structures, such finite elements would be highly desirable for large-scale analyses and design studies of high-performance aerospace vehicles.

Acknowledgments

The authors would like to thank Dr. Scott Burton of Avago Technologies for providing a research code that was used to compute the three-dimensional elasticity solutions for simply supported laminates. The first author is also very thankful to Prof. James G. Simmonds of the University of Virginia for a number of valuable technical discussions during the course of this research.

The second and third authors acknowledge the Piedmont Region for the financial support of this research in the framework of Contract E57 "Multidisciplinary optimization of aeromechanical structural systems." The third author also gratefully acknowledges Politecnico di Torino for supporting his research in the framework of the Young Researchers Program (2007).

Finally, the authors would like to thank the editorial committee of the Structural Mechanics and Concepts Branch of the NASA Langley Research Center, chaired by Dr. Michael P. Nemeth, for the many valuable suggestions.

References

[1] A. Tessler, "An Improved Plate Theory of {1,2}-Order for Thick Composite Laminates," International Journal of Solids and Structures, 30, 981-1000, 1993.

[2] G. M. Cook and A. Tessler, "A {3,2}-order Bending Theory for Laminated Composite and Sandwich Beams," Composites Part B: Engineering, 29, 565-576, 1998.

[3] A. Barut, E. Madenci, T. Anderson, and A. Tessler, "Equivalent Single Layer Theory for a Complete Stress Field in Sandwich Panels under Arbitrary Distributed Loading," Composite Structures, 58, 483-495, 2002.

[4] E. Reissner, "Reflections on the theory of elastic plates," Applied Mechanics Review, 38, 1453-1464, 1985.

[5] L. Librescu, A. A. Khdeir, and J. N. Reddy, "A comprehensive analysis of the state of stress of elastic anisotropic flat plates using refined theories," Acta Mechanica, 70, 57–81, 1987.

[6] A. K. Noor and W. S. Burton, "Assessment of shear deformable theories for multilayered composite plates," Applied Mechanics Review, 42, 1–12, 1989.

[7] D. Liu and X. Li, "An overall view of laminate theories based on displacement hypothesis," Journal of Composite Materials, 30(14), 1539-1561, 1996.

[8] S. A. Ambartsumian, "Theory of anisotropic shells," NASA TTF-118, 1964.

[9] C. T. Sun and J. M. Whitney, "Theories for the dynamic response of laminated plates," AIAA Journal, 11(2), 178-183, 1973.

[10] J. N. Reddy, "Mechanics of laminated composite plates. Theory and analysis," CRC Press, Inc., 1997.

[11] K. H. Lo, R. M. Christensen, and E. M. Wu, "A higher-order theory of plate deformation: Part 1. Homogeneous plates; Part 2. Laminated plates," ASME Journal of Applied Mechanics, 44, 663–676, 1977.

[12] M. Di Sciuva, "A refinement of the transverse shear deformation theory for multilayered orthotropic plates," Proceedings of 7th AIDAA National Congress, 1983; also in "L'aerotecnica missili e spazio", 62, 84-92, 1984.

[13] M. Di Sciuva, "A refined transverse shear deformation theory for multilayered anisotropic plates," Atti Accademia delle Scienze di Torino, 118, 279-295, 1984.

[14] M. Di Sciuva, "Development of an anisotropic, multilayered, shear-deformable rectangular plate element," Computers and Structures, 21(4), 789-796, 1985.

[15] M. Di Sciuva, "Evaluation of some multilayered, shear-deformable plate elements," Proceedings of 26th Structures, Structural Dynamics and Materials Conference, AIAA/ASME/ASCE/AHS-Paper 85-0717, 394-400, 1985.

[16] M. Di Sciuva, "Bending, vibration and buckling of simply supported thick multilayered orthotropic plates: an evaluation of a new displacement model," Journal of Sound and Vibration, 105, 425-442, 1986.

[17] H. Murakami, "Laminated composite plate theory with improved in-plane responses," ASME Journal of Applied Mechanics, 53, 661-666, 1986.

[18] M. Di Sciuva, "An improved shear-deformation theory for moderately thick multilayered anisotropic shells and plates," ASME Journal of Applied Mechanics, 54, 589-596, 1987.

[19] M. Di Sciuva, "Further refinement in the transverse shear deformation theory for multilayered composite plates," Atti Accademia delle Scienze di Torino, 124(5-6), 248-268, 1990.

[20] M. Di Sciuva, "Multilayered anisotropic plate models with continuous interlaminar stresses," Composite Structures, 22(3), 149-168, 1992.

[21] R. C. Averill, "Static and dynamic response of moderately thick laminated beams with damage," Composites Engineering, 4(4), 381-395, 1994.

[22] M. Di Sciuva, M. Gherlone, and L. Librescu, "Implications of damaged interfaces and of other non-classical effects on the load carrying capacity of multilayered composite shallow shells," International Journal of Non-Linear Mechanics, 37, 851-867, 2002.

[23] R. C. Averill and Y. C. Yip, "Development of simple, robust finite elements based on refined theories for thick laminated beams," Computers and Structures, 59(3), 529-546, 2006.

[24] P. Umasree and K. Bhaskar, "Analytical solutions for flexure of clamped rectangular cross-ply plates using an accurate zig-zag type higher-order theory," Composite Structures, 74, 426-439, 2006.

[25] A. Tessler, M. Di Sciuva, and M. Gherlone, "Refinement of Timoshenko beam theory for composite and sandwich beams using zigzag kinematics," NASA-TP-2007-215086, National Aeronautics and Space Administration, Washington, D.C., 2007.

[26] G. Arfken, "Mathematical Methods for Physicists," Academic Press, Orlando, FL, 1985.

[27] N. J. Pagano, "Exact solutions for composite laminates in cylindrical bending," Journal of Composite Materials, 3, 398-411, 1969.

[28] A. K. Noor and W. S. Burton, "Three-dimensional solutions for antisymmetrically laminated anisotropic plates," Transactions of the ASME, 57, 182-188, 1990.

[29] MSC/MD-NASTRAN, "Reference Guide," Version 2006.0, MSC Software Corporation, Santa Ana, CA.

[30] S. Vlachoutsis, "Shear correction factors for plates and shells," International Journal for Numerical Methods in Engineering, 33, 1537-1552, 1992.

[31] S. J. Reddy and K. Vijayakumar, "Lamination-dependent shear deformation models for cylindrical bending of angle-ply laminates," Computers and Structures, 55 (4), 717-725, 1994.

[32] F. J. Plantema, "Sandwich construction: the bending and buckling of sandwich beams, plates, and shells," John Wiley & Sons, New York (USA), 1966.

[33] H. G. Allen, "Analysis and design of structural sandwich panels," Pergamon, Oxford (UK), 1969

[34] J. R. Vinson and R. L. Sierakowski, "The behavior of structures composed of composite materials," Nijhoff, Dordrecht (The Netherlands), 1987.

Appendix A. Plate stiffness coefficients

The stiffness coefficients in Eq. (24) are computed from the following expressions using the constitutive coefficients given in Eq. (3).

(1) Matrix $\mathbf{A} \equiv [A_{ij}]\,(i, j = 1-3)$, symmetric, (3x3):

$$\mathbf{A} \equiv \int_{-h}^{h} \mathbf{C}\, dz \tag{A.1}$$

(2) Matrix $\mathbf{B} \equiv [B_{ij}]\,(i = 1-3; j = 1-7)$, non-symmetric, (3x7) :

$$\mathbf{B} \equiv \int_{-h}^{h} \mathbf{C}\, \mathbf{B}_{\phi}\, dz \tag{A.2}$$

(3) Matrix $\mathbf{D} \equiv [D_{ij}]\,(i, j = 1-7)$, symmetric, (7x7) :

$$\mathbf{D} \equiv \int_{-h}^{h} \mathbf{B}_{\phi}^{\mathrm{T}} \mathbf{C}\, \mathbf{B}_{\phi}\, dz \tag{A.3}$$

(4) Matrix $\mathbf{G} \equiv [G_{ij}]\,(i, j = 1-4)$, symmetric, (4x4) :

$$\mathbf{G} \equiv \int_{-h}^{h} \mathbf{B}_{\beta}^{\mathrm{T}} \mathbf{Q}\, \mathbf{B}_{\beta}\, dz \tag{A.4}$$

where

$$\mathbf{C} \equiv \begin{bmatrix} C_{11} & C_{12} & C_{16} \\ C_{12} & C_{22} & C_{26} \\ C_{16} & C_{26} & C_{66} \end{bmatrix}^{(k)} \tag{A.5}$$

$$\mathbf{Q} \equiv \begin{bmatrix} Q_{22} & Q_{12} \\ Q_{12} & Q_{11} \end{bmatrix}^{(k)} \tag{A.6}$$

$$\mathbf{B}_{\phi} \equiv \begin{bmatrix} z & \phi_1^{(k)} & 0 & 0 & 0 & 0 & 0 \\ 0 & 0 & z & \phi_2^{(k)} & 0 & 0 & 0 \\ 0 & 0 & 0 & 0 & z & \phi_1^{(k)} & \phi_2^{(k)} \end{bmatrix} \tag{A.7}$$

$$\mathbf{B}_\beta \equiv \begin{bmatrix} 1 & \beta_2^{(k)} & 0 & 0 \\ 0 & 0 & 1 & \beta_1^{(k)} \end{bmatrix} \tag{A.8}$$

Appendix B. Gram-Schmidt polynomials

The Gram-Schmidt orthogonal polynomials [26] are widely used as shape functions for application to the Rayleigh-Ritz method. These functions can accommodate various kinematic boundary conditions and yield a diagonal mass matrix.

The procedure for constructing such polynomials is initially established for one-dimensional domains, whereas for two-dimensional applications, simple products of one-dimensional functions are used.

The general expression of a one-dimensional Gram-Schmidt polynomial $\chi(s)$, where $s \in [0,1]$ is a dimensionless axial coordinate, is

$$\chi_{p+1}(s) = \left(s - A_p\right)\chi_p(s) - B_p\chi_{p-1}(s) \tag{B.1}$$

where the coefficients A_p and B_p are computed from the expressions

$$A_p \equiv \frac{\int_0^1 s\chi_p{}^2(s)ds}{\int_0^1 \chi_p{}^2(s)ds}, \quad B_p \equiv \frac{\int_0^1 \chi_p{}^2(s)ds}{\int_0^1 \chi_{p-1}{}^2(s)ds} \tag{B.2}$$

The process of building these functions initiates with the first two polynomials

$$\begin{aligned} &\chi_0(s) = 0 \\ &\chi_1(s) = \mu_1(s)^{\Omega_1}\mu_2(s)^{\Omega_2} \end{aligned} \tag{B.3}$$

where

$$\begin{aligned} &\mu_1(s) \equiv s \\ &\mu_2(s) \equiv 1 - s \end{aligned} \tag{B.4}$$

The three exponent values $\Omega_i = (0,1,2)$ correspond, respectively, to the end condition of the function: 0 if the function does not vanish, 1 if the function vanishes, however, its first derivative does not vanish, and 2 if the function and its first derivative vanish.

The orthogonality of the Gram-Schmidt polynomials is manifested by the relationship

$$\int_0^1 \chi_p(s)\chi_q(s)ds = c_{pq}\delta_{pq} \tag{B.5}$$

where c_{pq} is a coefficient and δ_{pq} is the Kronecker's delta.

For the cantilevered plate examined in Section 6, the Gram-Schmidt polynomials employed for the kinematic variables have the form

$$f\left(x_1, x_2\right) = \sum_{i=1}^{M} \sum_{j=1}^{N} f_{ij} \chi_i(x_1) \chi_j(x_2) \tag{B.6}$$

where M=7, N=5, and f_{ij} are the unknown amplitude coefficients to be determined from the Rayleigh-Ritz analysis.

$$\left.\begin{array}{l}\Omega_1 = 1 \\ \Omega_2 = 0\end{array}\right\} \begin{cases} \chi_1(\underline{x_1}) = \underline{x_1} \\ \chi_2(\underline{x_1}) = \underline{x_1^2} - \frac{3}{4}\underline{x_1} \\ \chi_3(\underline{x_1}) = \underline{x_1^3} - \frac{4}{3}\underline{x_1^2} + \frac{2}{5}\underline{x_1} \\ \chi_4(\underline{x_1}) = \underline{x_1^4} - \frac{15}{8}\underline{x_1^3} + \frac{15}{14}\underline{x_1^2} - \frac{5}{28}\underline{x_1} \\ \chi_5(\underline{x_1}) = \underline{x_1^5} - \frac{12}{5}\underline{x_1^4} + 2\underline{x_1^3} - \frac{2}{3}\underline{x_1^2} + \frac{1}{14}\underline{x_1} \\ \chi_6(\underline{x_1}) = \underline{x_1^6} - \frac{35}{12}\underline{x_1^5} + \frac{35}{11}\underline{x_1^4} - \frac{35}{22}\underline{x_1^3} + \frac{35}{99}\underline{x_1^2} - \frac{7}{264}\underline{x_1} \\ \chi_7(\underline{x_1}) = \underline{x_1^7} - \frac{24}{7}\underline{x_1^6} + \frac{60}{13}\underline{x_1^5} - \frac{40}{13}\underline{x_1^4} + \frac{150}{143}\underline{x_1^3} - \frac{24}{143}\underline{x_1^2} + \frac{4}{429}\underline{x_1} \end{cases} \tag{B.7}$$

$$\left.\begin{array}{l}\Omega_1 = 0 \\ \Omega_2 = 0\end{array}\right\} \begin{cases} \chi_1(\underline{x_2}) = 1 \\ \chi_2(\underline{x_2}) = \underline{x_2} - \frac{1}{2} \\ \chi_3(\underline{x_2}) = \underline{x_2^2} - \underline{x_2} + \frac{1}{6} \\ \chi_4(\underline{x_2}) = \underline{x_2^3} - \frac{3}{2}\underline{x_2^2} + \frac{3}{5}\underline{x_2} - \frac{1}{20} \\ \chi_5(\underline{x_2}) = \underline{x_2^4} - 2\underline{x_2^3} + \frac{9}{7}\underline{x_2^2} - \frac{2}{7}\underline{x_2} + \frac{1}{70} \end{cases} \tag{B.8}$$

with

$$\underline{x_1} \equiv x_1 / a$$
$$\underline{x_2} \equiv x_2 / b \tag{B.9}$$

For the simply supported angle-ply antisymmetric laminates considered in Section 6, the Di Sciuva zigzag theory solutions utilizing the Rayleigh-Ritz method employ the Gram-Schmidt polynomials corresponding to M=N=5. Because the kinematic variables have different boundary conditions, Eq. (26.1-a) and Eq. (26.2-a), the Gram-Schmidt polynomials are chosen according to the table below.

Table B. Parameters for Gram-Schmidt polynomials.

Kinematic variable	$\chi_i(x_1)$		$\chi_i(x_2)$	
	Ω_1	Ω_2	Ω_1	Ω_2
u	1	1	0	0
v	0	0	1	1
w	1	1	1	1
ψ_1	0	0	1	1
ψ_2	1	1	0	0

For example, the x_1-direction functions for the transverse displacement, w, have the form,

$$\Omega_1 = 1,\ \Omega_2 = 1 \quad \begin{cases} \chi_1(\underline{x_1}) = \underline{x_1^2} - \underline{x_1} \\ \chi_2(\underline{x_1}) = \underline{x_1^3} - \frac{3}{2}\underline{x_1^2} + \frac{1}{2}\underline{x_1} \\ \chi_3(\underline{x_1}) = \underline{x_1^4} - 2\underline{x_1^3} + \frac{17}{14}\underline{x_1^2} - \frac{3}{14}\underline{x_1} \\ \chi_4(\underline{x_1}) = \underline{x_1^5} - \frac{5}{2}\underline{x_1^4} + \frac{13}{6}\underline{x_1^3} - \frac{3}{4}\underline{x_1^2} + \frac{1}{12}\underline{x_1} \\ \chi_5(\underline{x_1}) = \underline{x_1^6} - 3\underline{x_1^5} + \frac{37}{11}\underline{x_1^4} - \frac{19}{11}\underline{x_1^3} + \frac{13}{33}\underline{x_1^2} - \frac{1}{33}\underline{x_1} \end{cases} \tag{B.10}$$

Similar functions are constructed for the x_2-direction.

Table 1. Mechanical material properties.

Orthotropic materials			Isotropic materials		
Lamina material	C	H	Lamina material	P	T
	Carbon-Epoxy unidirectional composite	Titanium honeycomb core		PVC core	Titanium
$E_1^{(k)}$ [GPa]	1.579×10^{2}	1.915×10^{-1}	$E^{(k)}$ [GPa]	1.040×10^{-1}	1.041×10^{2}
$E_2^{(k)}$ [GPa]	9.584	1.915×10^{-1}			
$E_3^{(k)}$ [GPa]	9.584	1.915			
$\nu_{12}^{(k)}$	0.32	0.658×10^{-2}	$\nu^{(k)}$	0.3	0.31
$\nu_{13}^{(k)}$	0.32	0.643×10^{-6}			
$\nu_{23}^{(k)}$	0.49	0.643×10^{-6}			
$G_{12}^{(k)}$ [GPa]	5.930	4.227×10^{-8}			
$G_{13}^{(k)}$ [GPa]	5.930	5.651×10^{-1}			
$G_{23}^{(k)}$ [GPa]	3.227	1.248			

Table 2. Laminate stacking sequences (lamina sequence is in the positive z direction).

Laminate		Normalized lamina thickness, $h^{(k)}/h$	Lamina materials	Lamina orientation [°]
A	Cross-ply composite	(0.5/0.5)	(C/C)	(0/90)
B	Uniaxial sandwich	(0.1/0.8/0.1)	(C/P/C)	(0/0/0)
B_1	Uniaxial sandwich	(0.025/0.95/0.025)	(C/P/C)	(0/0/0)
B_2	Uniaxial sandwich	(0.0025/0.995/0.0025)	(C/P/C)	(0/0/0)
F	Uniaxial sandwich	(0.1/0.8/0.1)	(T/H/T)	(0/0/0)
G	Angle-ply sandwich	(0.05/0.05/0.8/0.05/0.05)	(C/C/P/C/C)	(30/-45/0/45/-30)

Table 3. Normalized maximum (central) deflection, $\bar{w} = (10^2 D_{11}/q_o a^4)\, w(a/2, b/2)$, for simply supported laminates subjected to sinusoidal transverse pressure loading.

Laminate	Normalization factor, $10^2 D_{11}/q_o a^4$	3D Elasticity	FSDT	Zigzag (D)	Zigzag (R)
A	8.147×10^{-2}	1.228	1.278	1.170	1.219
B	7.502×10^{-2}	29.761	2.731	29.769	29.785
B_1	2.201×10^{-2}	11.645	2.819	11.693	11.694
B_2	2.402×10^{-3}	2.080	1.728	2.103	2.103
F	5.444×10^{-2}	1.331	0.389	1.332	1.333
G	3.551×10^{-2}	14.124	1.055	12.734	14.105

Table 4. Normalized maximum (top surface) displacement along x_1 axis $\bar{u}_1 = (10^3 D_{11}/q_o a^4) \times u_1^{(N)}(a, b/2, h)$ of simply supported laminates subjected to sinusoidal transverse pressure loading.

Laminate	Normalization factor, $10^3 D_{11}/q_o a^4$	3D Elasticity	FSDT	Zigzag (D)	Zigzag (R)
A	8.147×10^{-1}	4.233	4.152	3.855	4.251
B	7.502×10^{-1}	9.977	2.156	9.945	9.897
B1	2.201×10^{-1}	2.008	2.099	2.030	2.032
B2	2.402×10^{-2}	1.809	1.993	1.851	1.851
F	5.444×10^{-1}	0.643	0.796	0.646	0.649
G	3.551×10^{-1}	3.908	0.704	1.295	3.845

Table 5. Normalized maximum (central) deflection, $\bar{w} = (10^2 D_{11}/q_o a^4)\, w(a/2, b/2)$, for simply supported laminate B subjected to sinusoidal transverse pressure loading and corresponding to various span-to-thickness ratios.

Span-to-thickness ratio	Normalization factor, $10^2 D_{11}/q_o a^4$	3D Elasticity	FSDT	Zigzag (D)	Zigzag (R)
4	1.832×10^{-1}	42.420	3.739	42.124	42.189
10	4.668×10^{-3}	9.734	1.321	9.738	9.739
20	2.931×10^{-4}	3.487	0.948	3.489	3.490
50	7.502×10^{-6}	1.305	0.841	1.305	1.305
100	4.688×10^{-7}	0.945	0.826	0.945	0.945
200	2.931×10^{-8}	0.852	0.822	0.852	0.852

Table 6. Normalized maximum (free-edge) deflection, $\bar{w} = (10^2 D_{11} / q_o a^4)\, w(a, b/2)$, for cantilevered laminate B subjected to uniform transverse pressure loading.

Normalization factor, $10^2 D_{11} / q_o a^4$	3D FEM	FSDT	Zigzag (D)	Zigzag (R)
7.502×10^{-2}	246.778	25.351	244.077	245.615

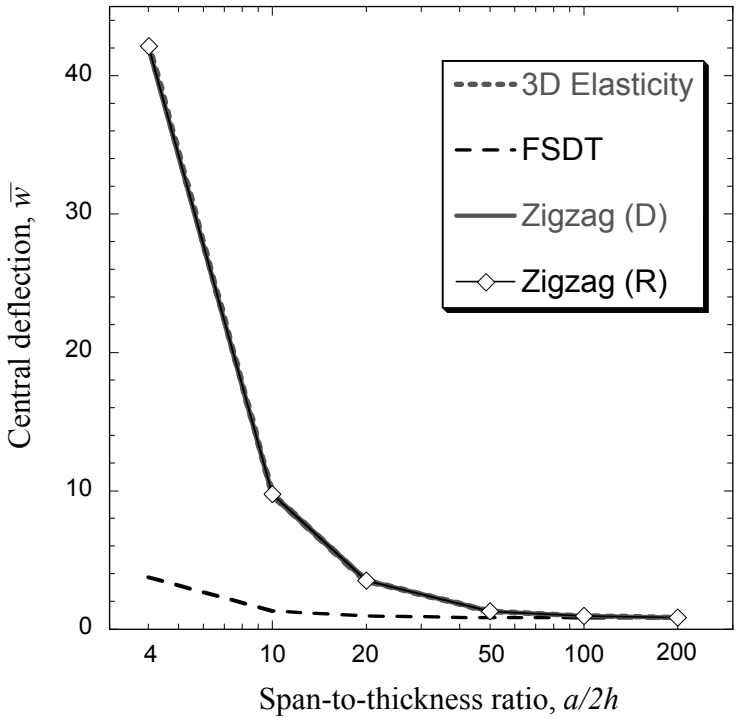

Figure 3 (a). Normalized central deflection vs. span-to-thickness ratio for simply supported laminate B subjected to sinusoidal transverse pressure.

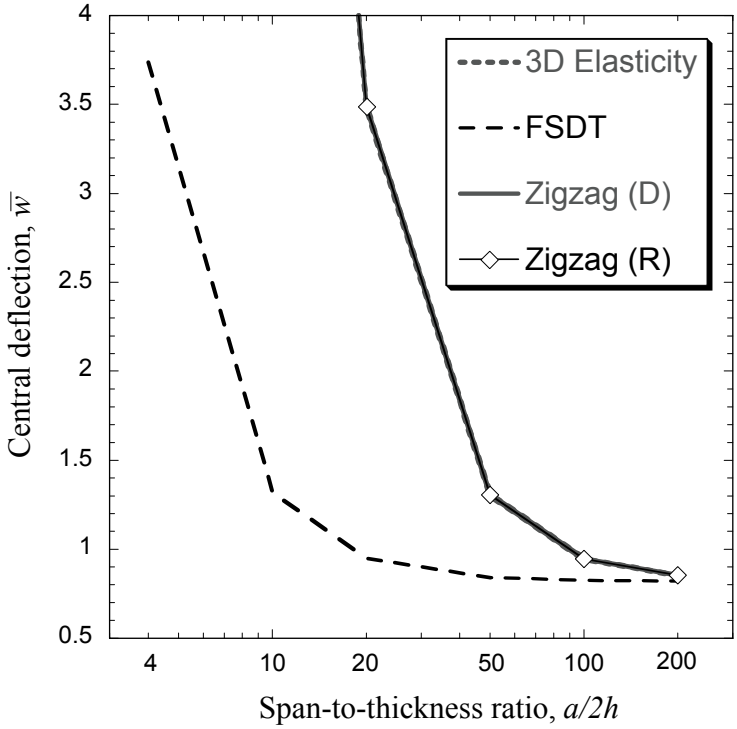

Figure 3 (b). Normalized central deflection vs. span-to-thickness ratio for simply supported laminate B subjected to sinusoidal transverse pressure (zoomed view).

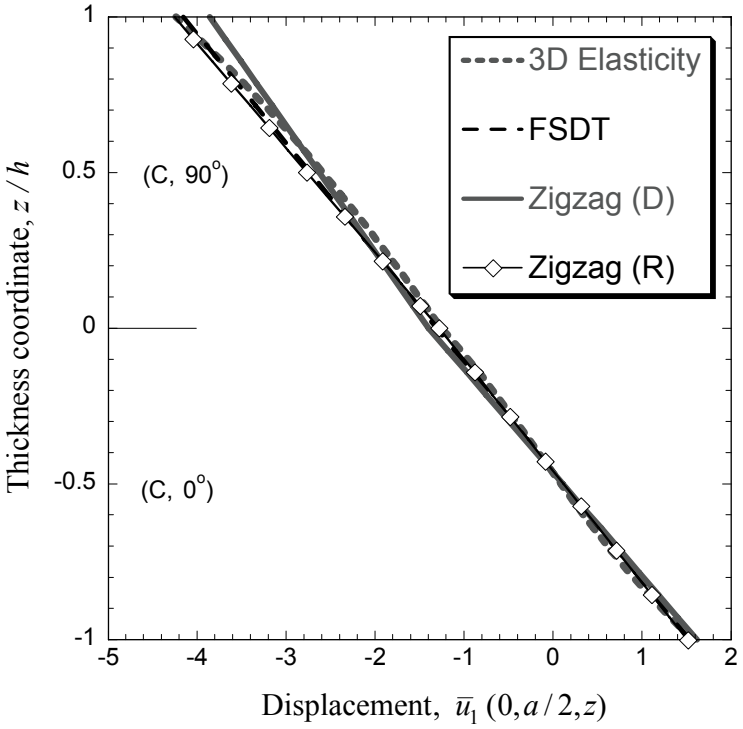

Figure 4. Normalized in-plane displacement for simply supported laminate A subjected to sinusoidal transverse pressure.

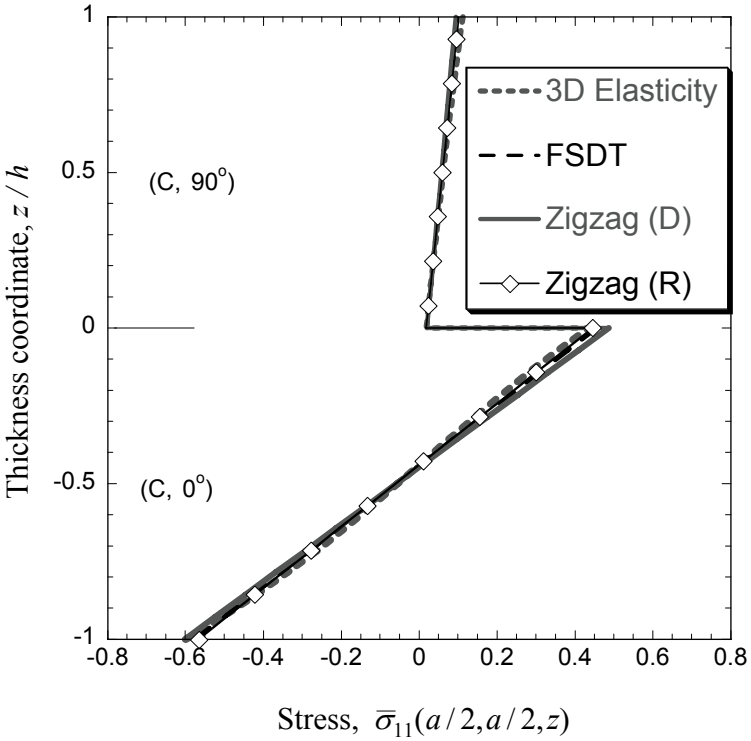

Figure 5. Normalized normal stress for simply supported laminate A subjected to sinusoidal transverse pressure.

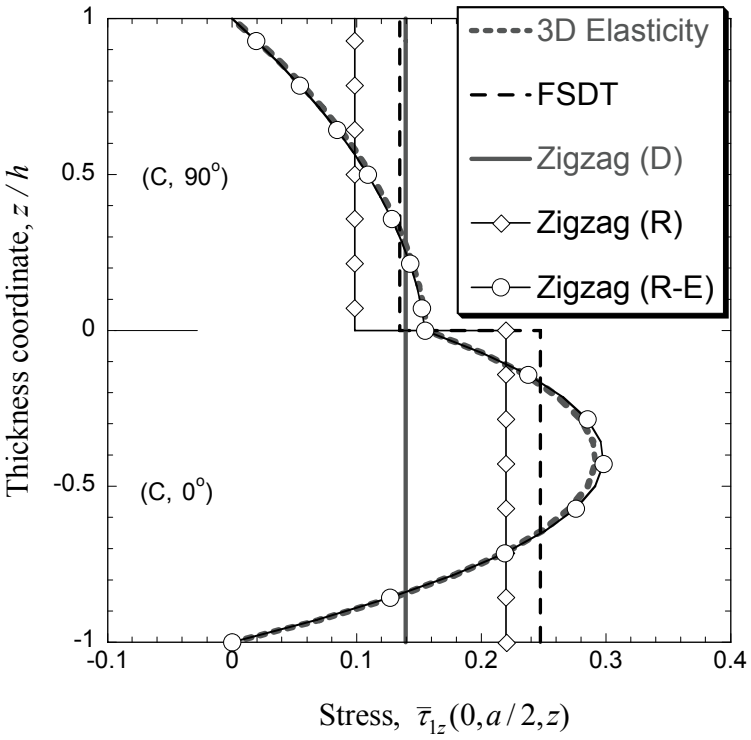

Figure 6. Normalized transverse shear stress for simply supported laminate A subjected to sinusoidal transverse pressure.

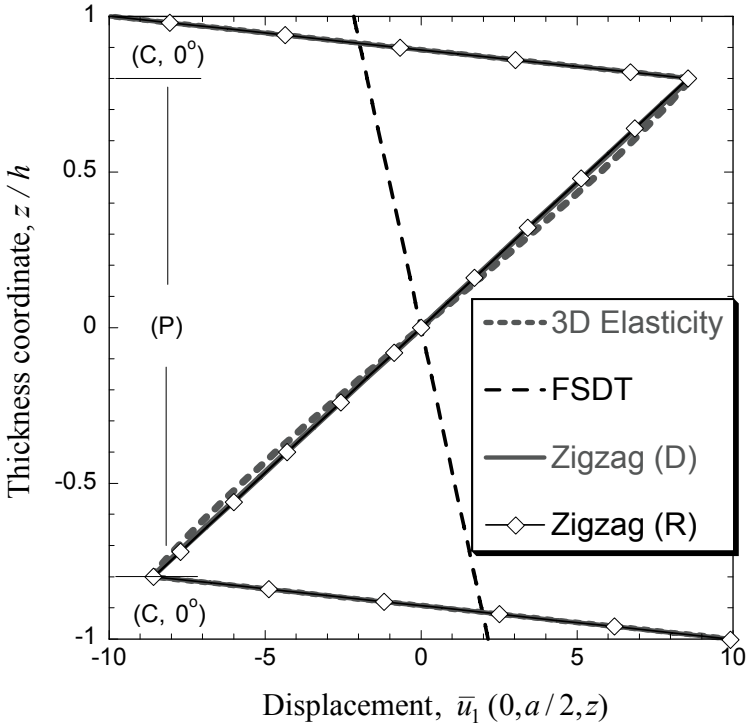

Figure 7. Normalized in-plane displacement for simply supported laminate B subjected to sinusoidal transverse pressure.

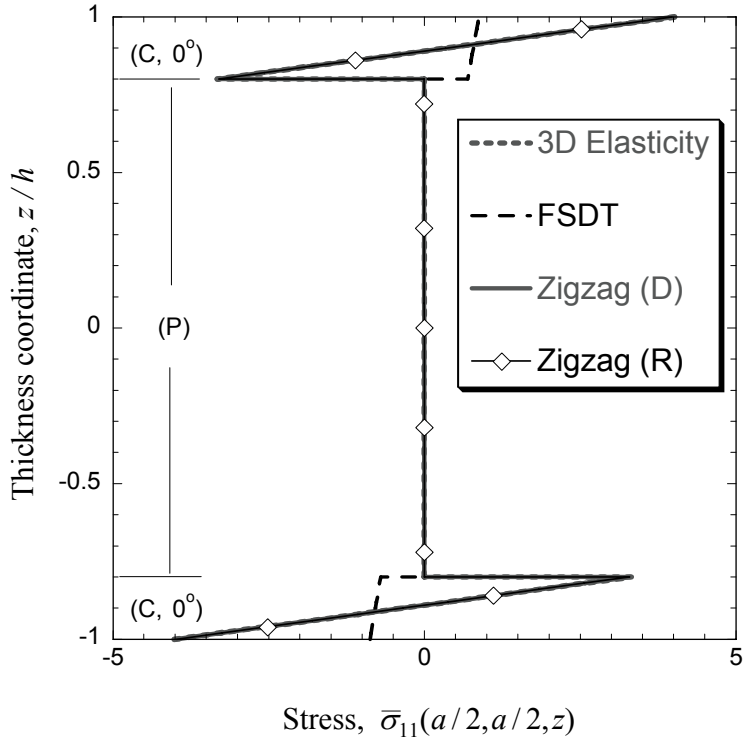

Figure 8. Normalized normal stress for simply supported laminate B subjected to sinusoidal transverse pressure.

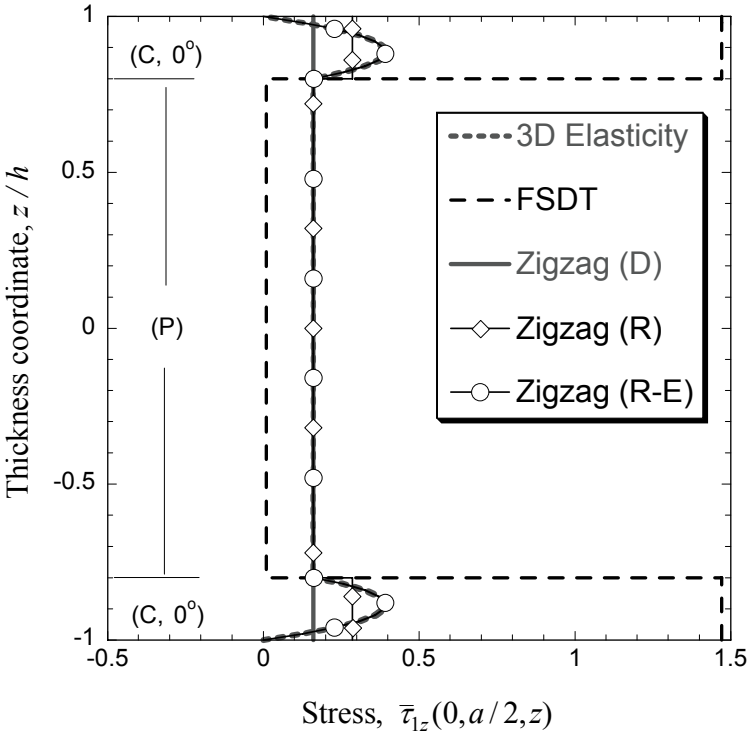

Figure 9. Normalized transverse shear stress for simply supported laminate B subjected to sinusoidal transverse pressure.

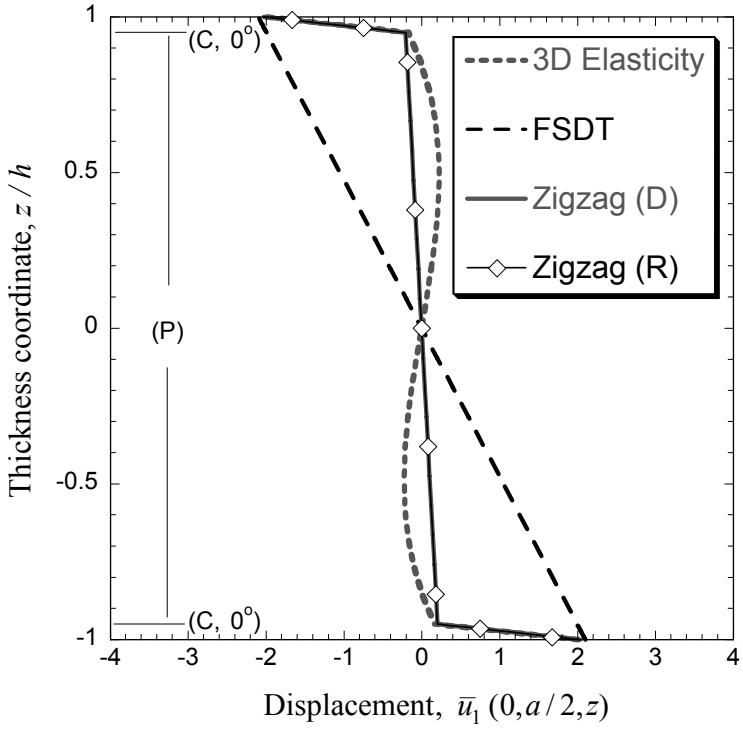

Figure 10. Normalized in-plane displacement for simply supported laminate B_1 subjected to sinusoidal transverse pressure.

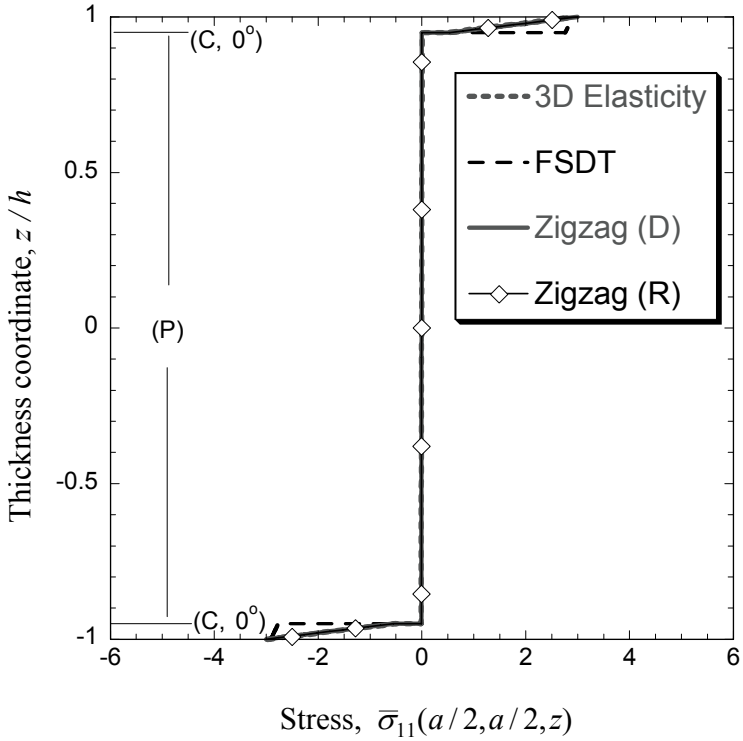

Figure 11 (a). Normalized normal stress for simply supported laminate B_1 subjected to sinusoidal transverse pressure.

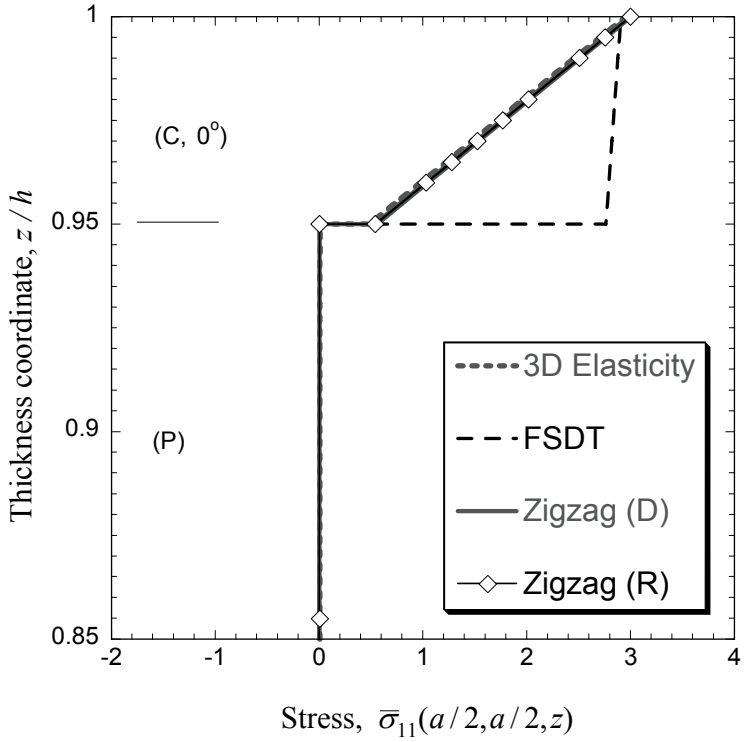

Figure 11 (b). Normalized normal stress near the top layer for simply supported laminate B_1 subjected to sinusoidal transverse pressure.

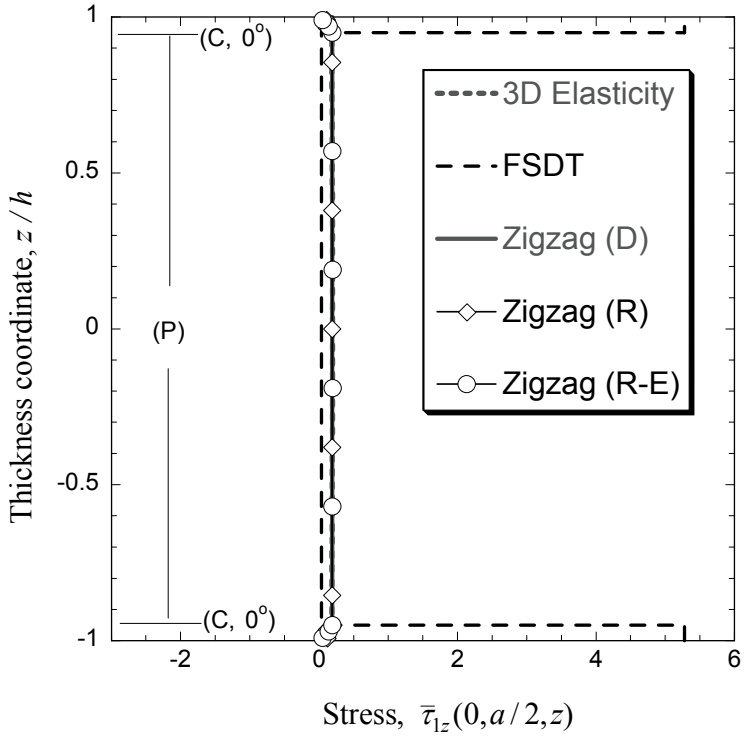

Figure 12 (a). Normalized transverse shear stress for simply supported laminate B_1 subjected to sinusoidal transverse pressure.

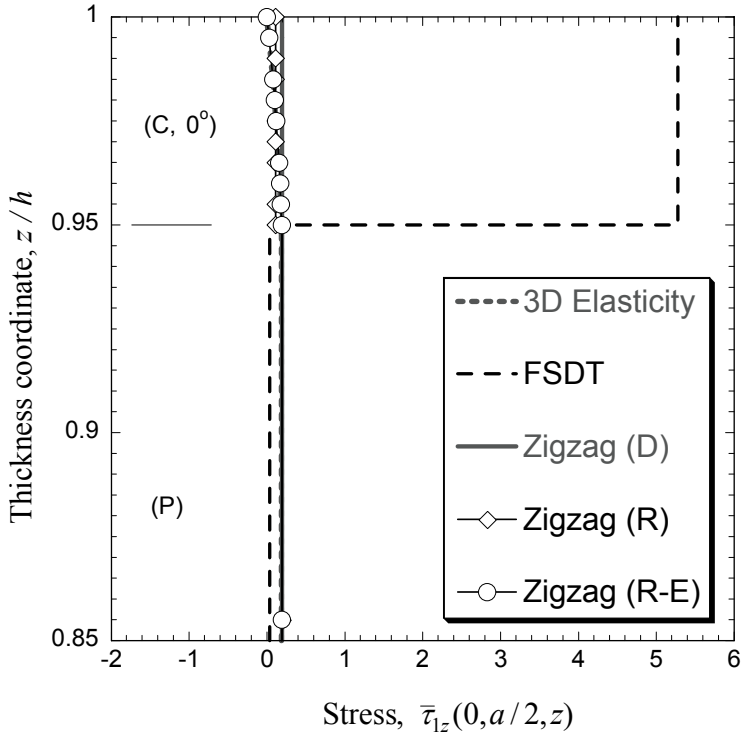

Figure 12 (b). Normalized transverse shear stress near the top layer for simply supported laminate B_1 subjected to sinusoidal transverse pressure.

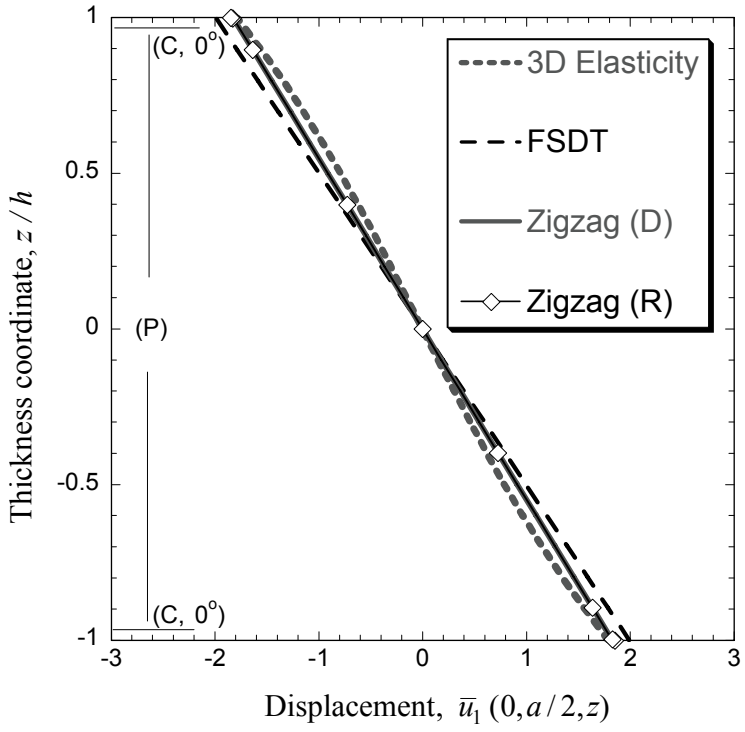

Figure 13. Normalized in-plane displacement for simply supported laminate B2 subjected to sinusoidal transverse pressure.

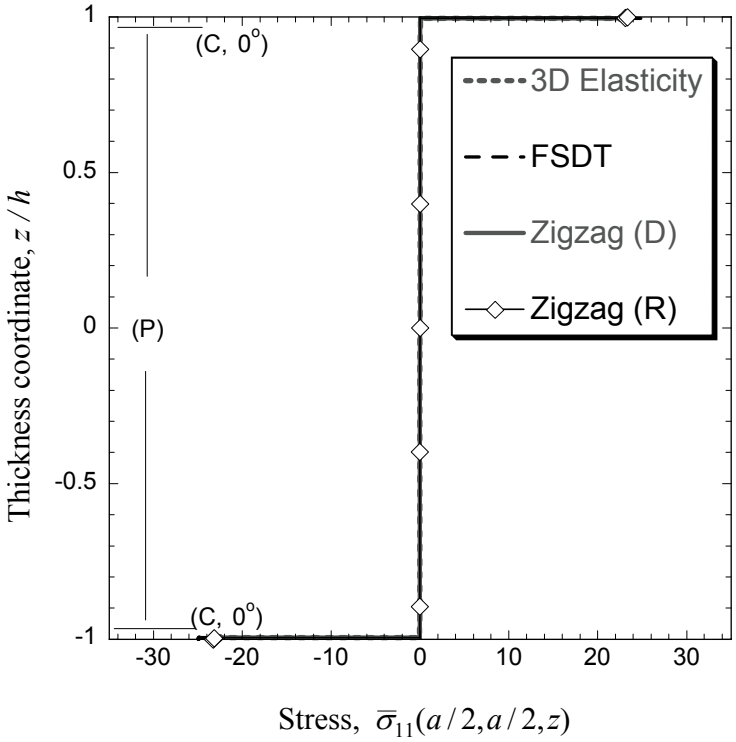

Figure 14 (a). Normalized normal stress for simply supported laminate B_2 subjected to sinusoidal transverse pressure.

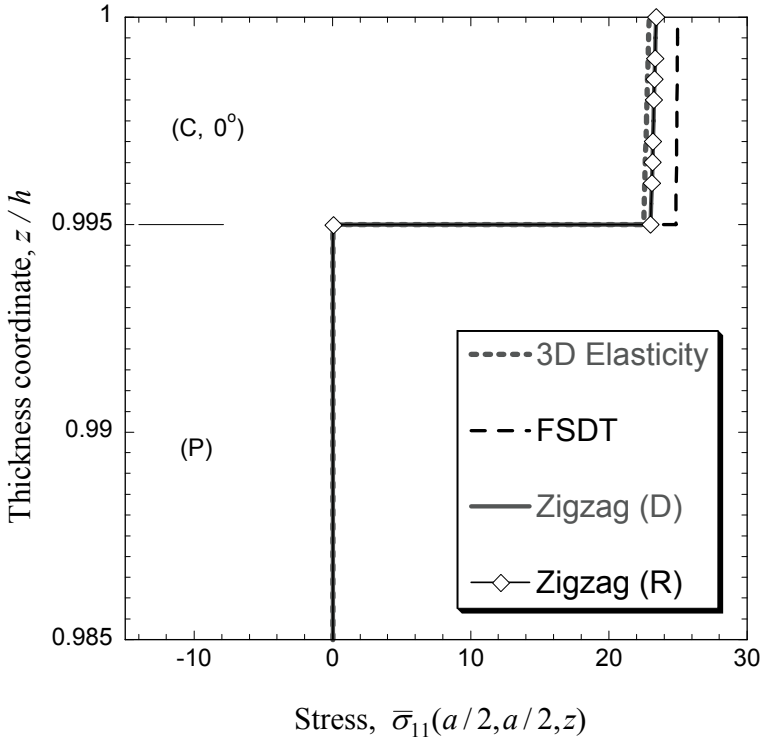

Figure 14 (b). Normalized normal stress near the top layer for simply supported laminate B_2 subjected to sinusoidal transverse pressure.

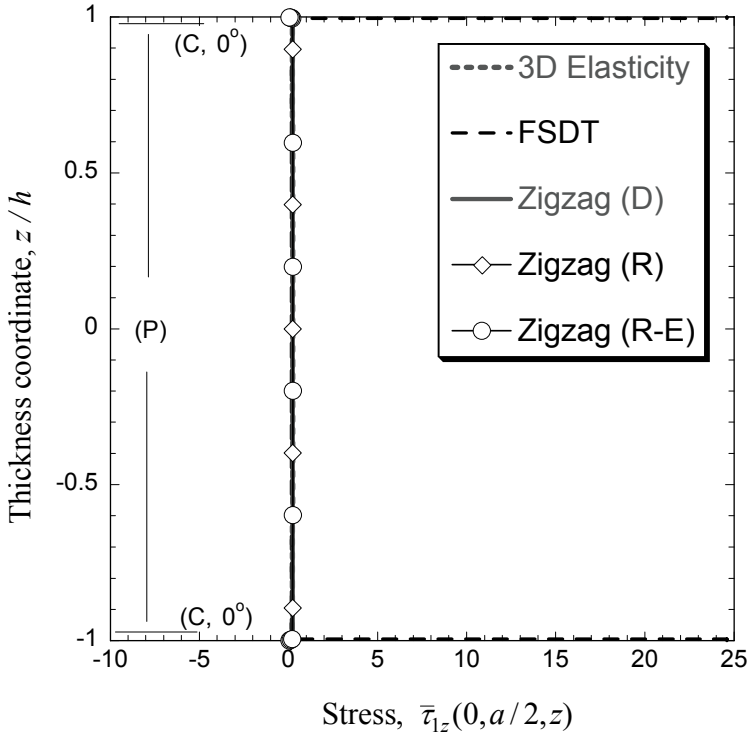

Figure 15 (a). Normalized transverse shear stress for simply supported laminate B_2 subjected to sinusoidal transverse pressure.

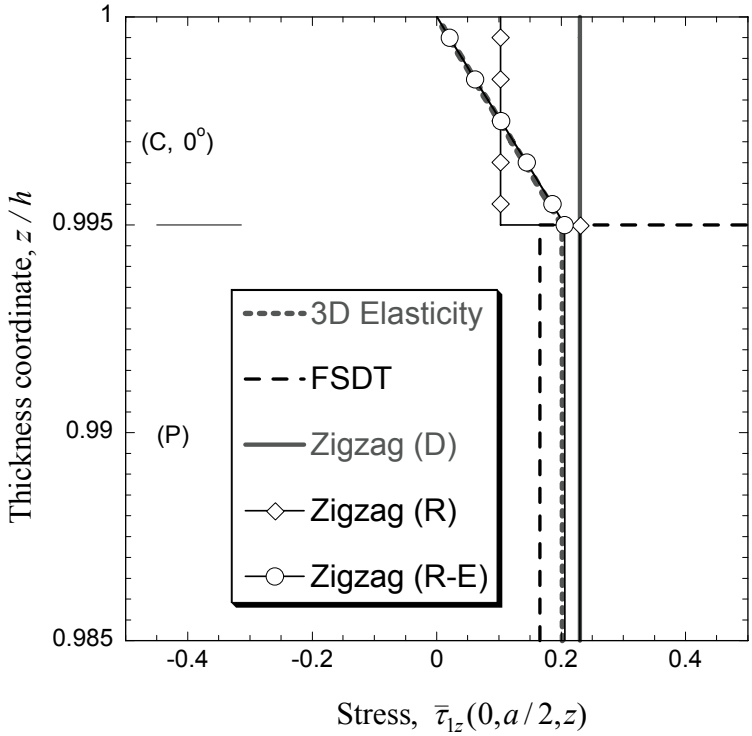

Figure 15 (b). Normalized transverse shear stress near the top layer for simply supported laminate B_2 subjected to sinusoidal transverse pressure.

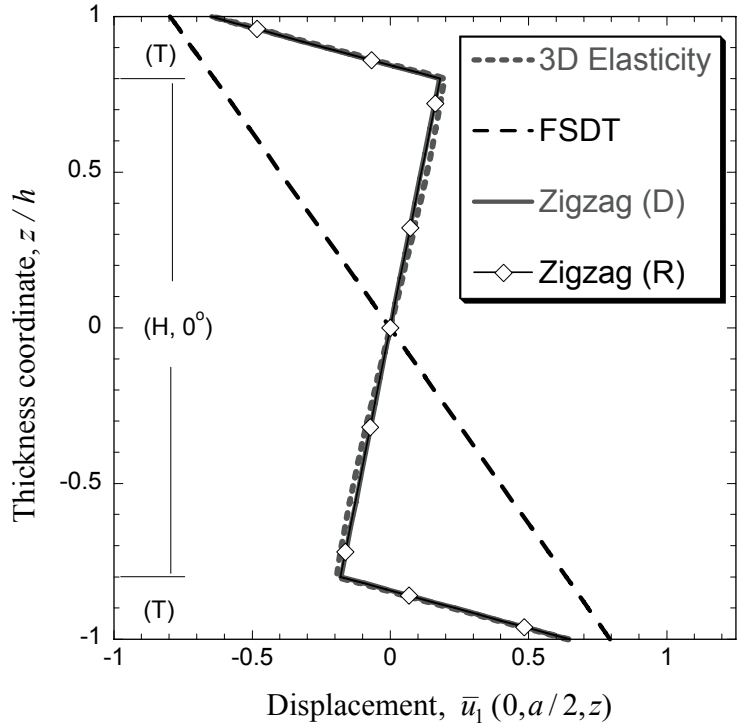

Figure 16. Normalized in-plane displacement for simply supported laminate F subjected to sinusoidal transverse pressure.

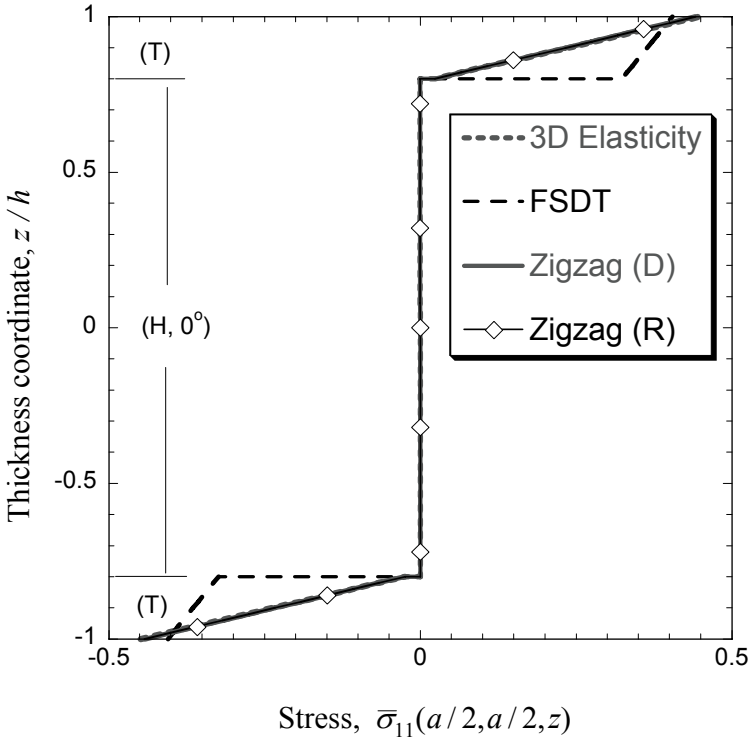

Figure 17. Normalized normal stress for simply supported laminate F subjected to sinusoidal transverse pressure.

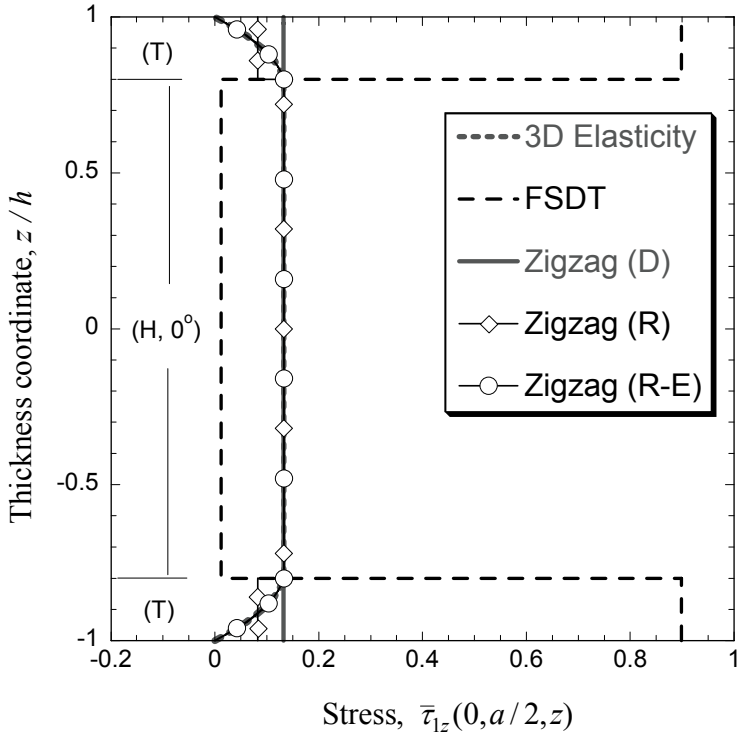

Figure 18 (a). Normalized transverse shear stress for simply supported laminate F subjected to sinusoidal transverse pressure.

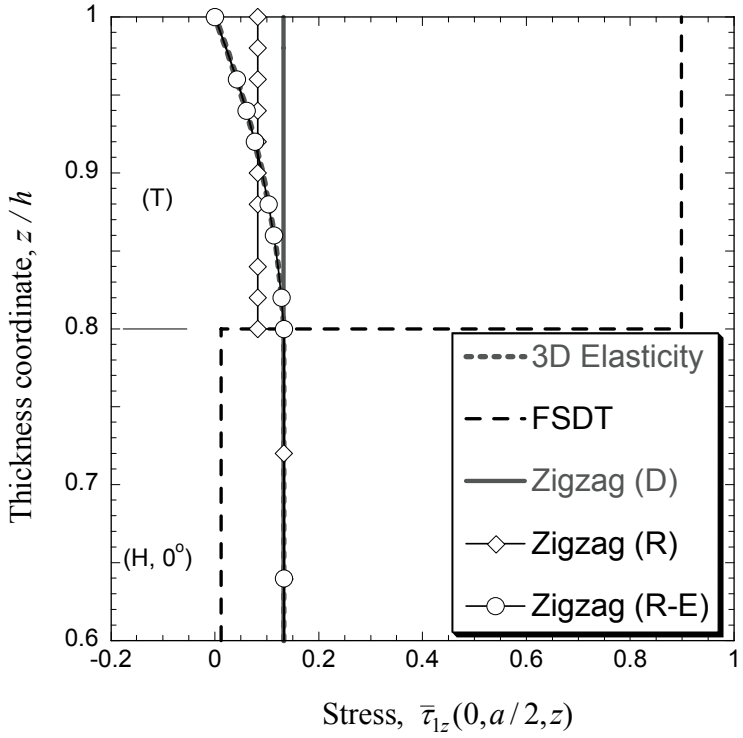

Figure 18 (b). Normalized transverse shear stress near the top layer for simply supported laminate F subjected to sinusoidal transverse pressure.

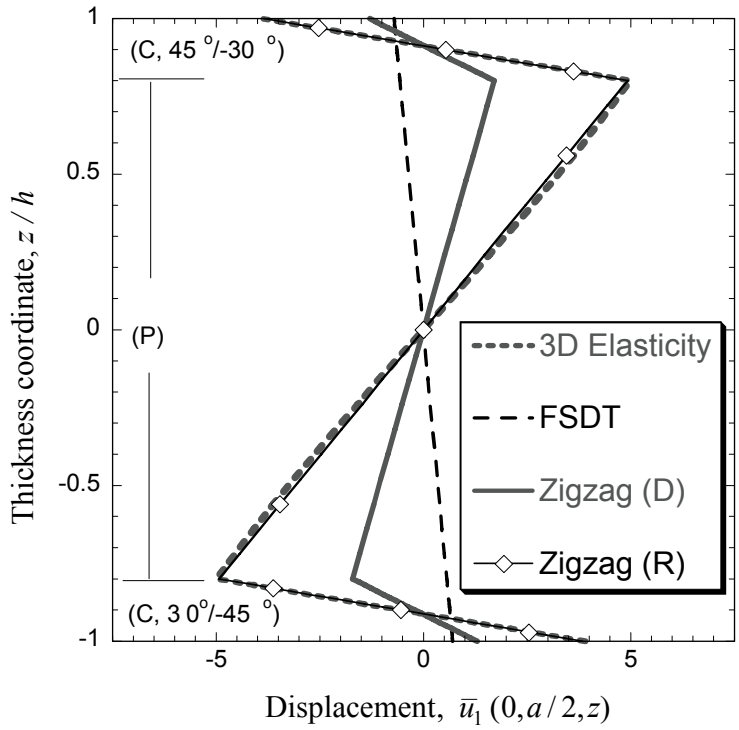

Figure 19. Normalized in-plane displacement for simply supported laminate G subjected to sinusoidal transverse pressure.

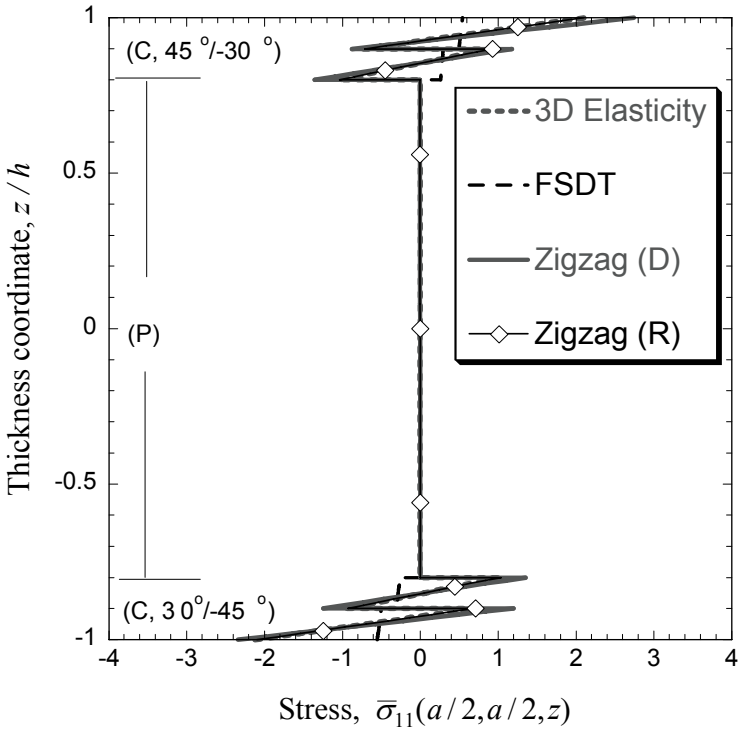

Figure 20. Normalized normal stress for simply supported laminate G subjected to sinusoidal transverse pressure.

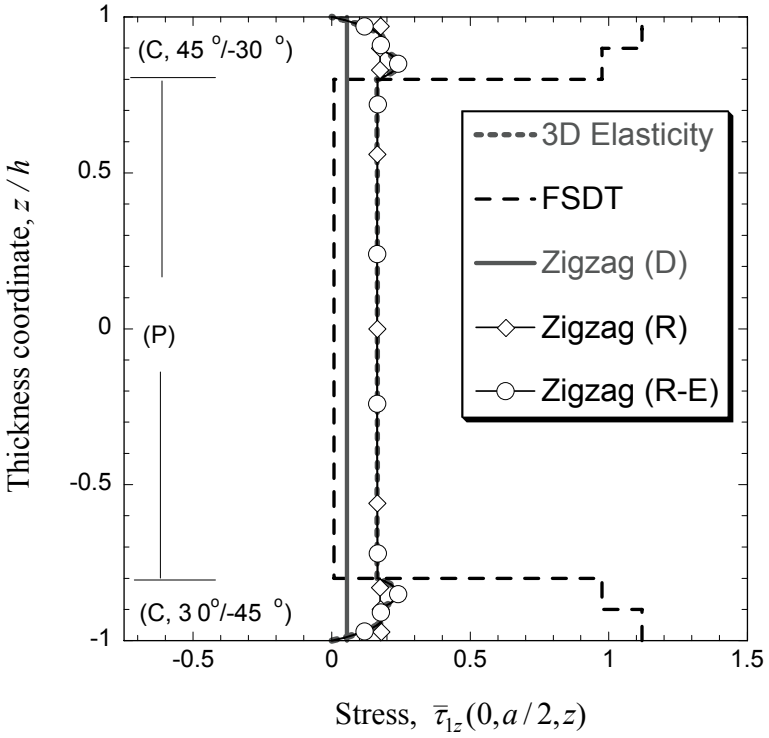

Figure 21 (a). Normalized transverse shear stress for simply supported laminate G subjected to sinusoidal transverse pressure.

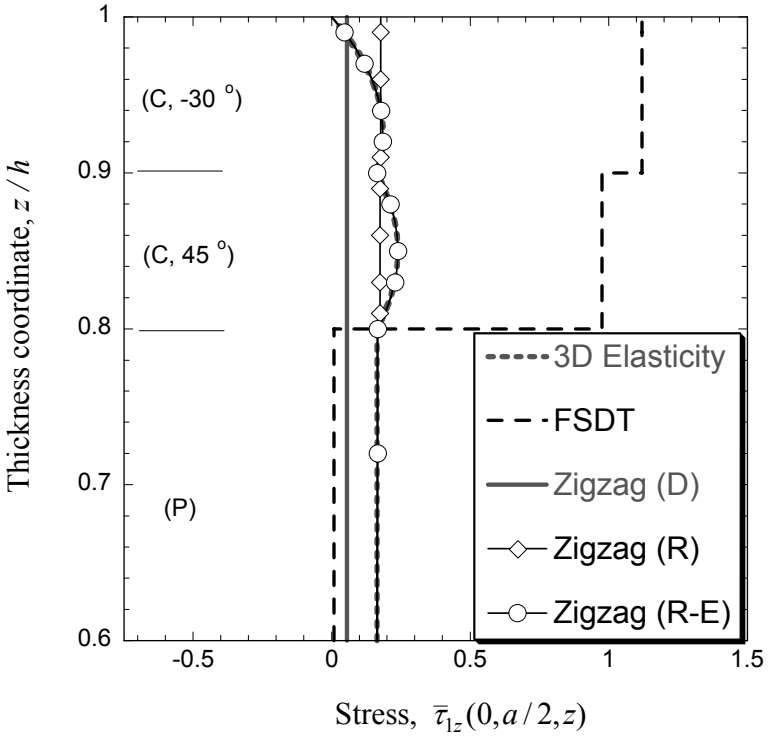

Figure 21 (b). Normalized transverse shear stress near the top layer for simply supported laminate G subjected to sinusoidal transverse pressure.

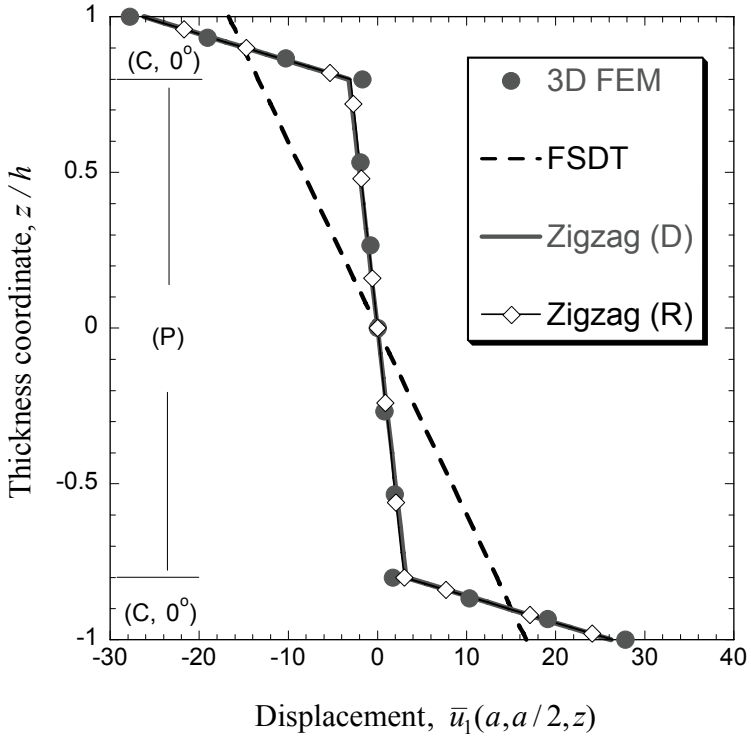

Figure 22. Normalized in-plane displacement for cantilevered laminate B subjected to uniform transverse pressure.

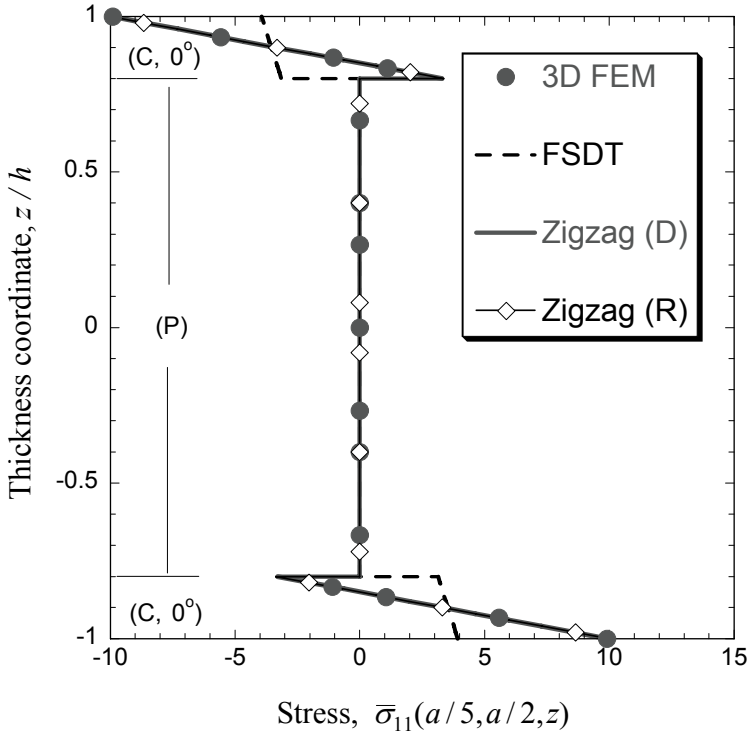

Figure 23. Normalized normal stress for cantilevered laminate B subjected to uniform transverse pressure.

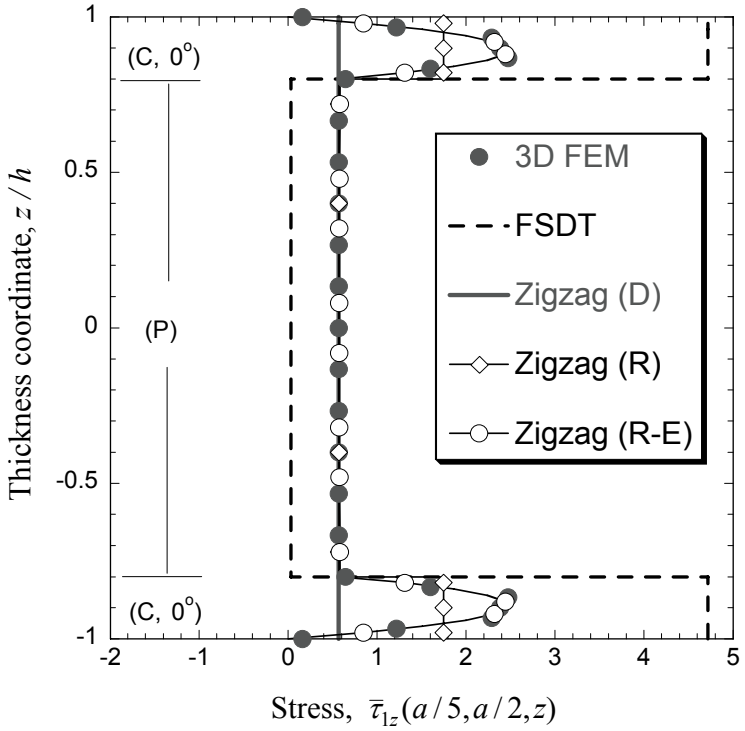

Figure 24 (a). Normalized transverse shear stress for cantilevered laminate B subjected to uniform transverse pressure.

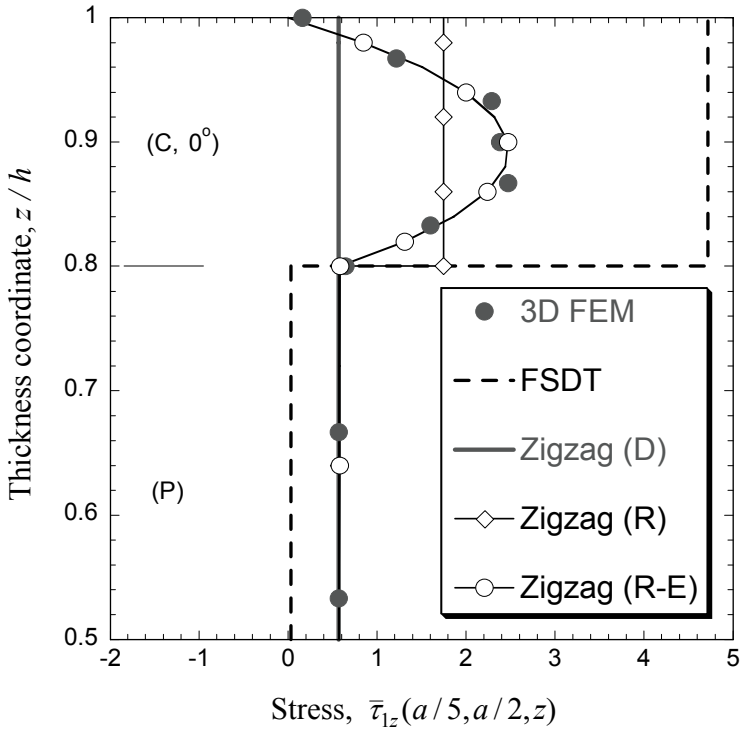

Figure 24 (b). Normalized transverse shear stress for cantilevered laminate B subjected to uniform transverse pressure.

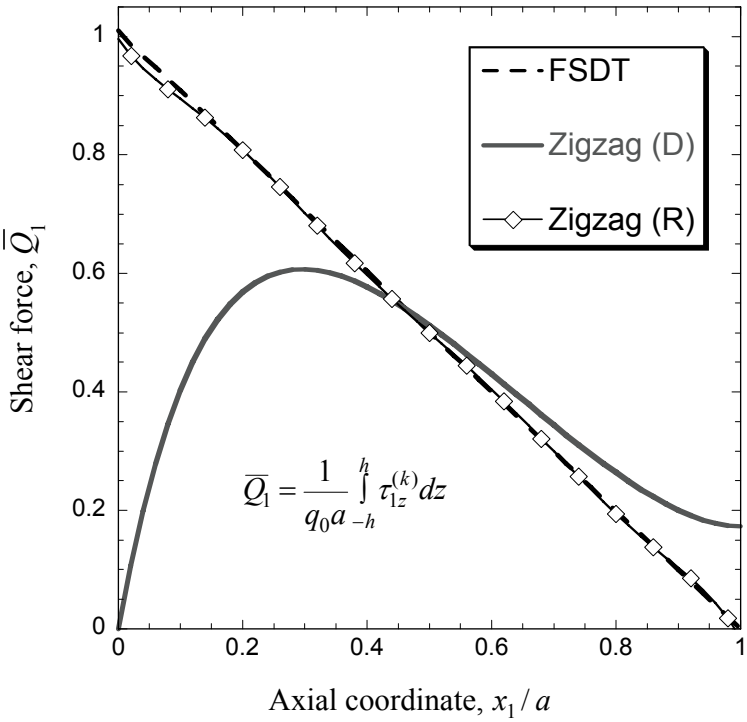

Figure 25. Normalized transverse shear force along centerline of cantilevered laminate B subjected to uniform transverse pressure.

REPORT DOCUMENTATION PAGE

Form Approved
OMB No. 0704-0188

1. REPORT DATE *(DD-MM-YYYY)*	2. REPORT TYPE	3. DATES COVERED *(From - To)*
01- 01 - 2009	Technical Publication	

4. TITLE AND SUBTITLE
Refined Zigzag Theory for Laminated Composite and Sandwich Plates

5a. CONTRACT NUMBER

5b. GRANT NUMBER

5c. PROGRAM ELEMENT NUMBER

6. AUTHOR(S)
Tessler, Alexander; Di Sciuva, Marco; Gherlone, Marco

5d. PROJECT NUMBER

5e. TASK NUMBER

5f. WORK UNIT NUMBER
984754.02.07.07.15.04

7. PERFORMING ORGANIZATION NAME(S) AND ADDRESS(ES)
NASA Langley Research Center
Hampton, VA 23681-2199

Dept. of Aeronautics and Space Engineering
Politecnico di Torino
Corso Duca degli Abruzzi, 24
10129, Torino, Italy

8. PERFORMING ORGANIZATION REPORT NUMBER
L-19564

9. SPONSORING/MONITORING AGENCY NAME(S) AND ADDRESS(ES)
National Aeronautics and Space Administration
Washington, DC 20546-0001

10. SPONSOR/MONITOR'S ACRONYM(S)
NASA

11. SPONSOR/MONITOR'S REPORT NUMBER(S)
NASA/TP-2009-215561

12. DISTRIBUTION/AVAILABILITY STATEMENT
Unclassified - Unlimited
Subject Category 24
Availability: NASA CASI (443) 757-5802

13. SUPPLEMENTARY NOTES

14. ABSTRACT

A refined zigzag theory is presented for laminated-composite and sandwich plates that includes the kinematics of first-order shear-deformation theory as its baseline. The theory is variationally consistent and is derived from the virtual work principle. Novel piecewise-linear zigzag functions that provide a more realistic representation of the deformation states of transverse-shear-flexible plates than other similar theories are used. The formulation does not enforce full continuity of the transverse shear stresses across the plate's thickness, yet is robust. Transverse-shear correction factors are not required to yield accurate results. The theory is devoid of the shortcomings inherent in the previous zigzag theories including shear-force inconsistency and difficulties in simulating clamped boundary conditions. This new theory requires only C0-continuous kinematic approximations and is perfectly suited for developing computationally efficient finite elements. The theory should be useful for obtaining relatively efficient, accurate estimates of structural response needed to design high-performance load-bearing aerospace structures.

15. SUBJECT TERMS
Plate theory; Laminated composites; Sandwich plates; Transverse shear deformation; Zigzag kinematics; Finite element method; Virtual work principle

16. SECURITY CLASSIFICATION OF:			17. LIMITATION OF ABSTRACT	18. NUMBER OF PAGES	19a. NAME OF RESPONSIBLE PERSON
a. REPORT	b. ABSTRACT	c. THIS PAGE			STI Help Desk (email: help@sti.nasa.gov)
					19b. TELEPHONE NUMBER *(Include area code)*
U	U	U	UU	53	(443) 757-5802